https://doi.org/10.5194/hess-2022-160
Preprint. Discussion started: 2 May 2022

Hydrology and Earth System Sciences
Open Access
Discussions

Climate warming-driven changes in the cryosphere and their impact on groundwater-surface water interactions in the Heihe River Basin

Amanda Triplett[1], Laura E. Condon[1]

[1]Hydrology and Atmospheric Sciences, The University of Arizona, Tucson, 85705, The United States of America

Correspondence to: Amanda Triplett (aktriplett@email.arizona.edu)

Abstract. The Heihe River Basin in Northwestern China depends heavily on both manmade and natural storage (e.g., surface reservoirs, rivers, and groundwater) to support economic and environmental functions. The Qilian Mountain cryosphere in the upper basin is integral to recharging these storage supplies. It is well established that climate warming is driving major shifts in high elevation water storage through loss of glaciers and permafrost. However, the impacts on groundwater-surface water interactions and water supply in corresponding lower reaches are less clear. We built an integrated hydrologic model of the middle-basin, where most water usage occurs in order to explore the hydrologic response to cryosphere trends. We simulate watershed response to loss of glaciers (*Glacier* scenario), advanced permafrost degradation (*Permafrost* scenario), both responses (*Combined* scenario) and projected temperature increases in the middle basin (*Warming* scenario) by altering streamflow inputs to the model to represent cryosphere melting processes, as well as by increasing the temperature of the climate forcing data. Net losses to groundwater storage in the *Glacier* scenario and net gains in *Permafrost* and *Combined* show the potential of groundwater exchanges to mediate streamflow shifts. The result of the *Combined* scenario also shows that permafrost degradation has more of an impact on the system than glacial loss. Seasonal differences in groundwater-surface water partitioning are also evident. The *Glacier* scenario has the highest fraction of groundwater in streamflow in early spring. The *Permafrost* and *Combined* scenarios meanwhile have the highest fraction of streamflow entering the subsurface in late spring and summer. The *Warming* scenario raises the temperature of the *Combined* scenario by 2C. A reversal in trend to net groundwater storage loss, and large seasonal changes in evapotranspiration and stream network connectivity relative to *Combined* show the potential for warming to overpower changes resulting from streamflow. Our results demonstrate the importance of understanding the entire system of groundwater-surface water exchanges to assess water resources under changing climatic conditions. Ultimately, this analysis can be used to examine the cascading impact of climate change in the cryosphere on the resilience of water resources in arid basins downstream of mountain ranges globally.

1 Introduction

Mountains are an important source of freshwater for arid regions around the world (Qin et al., 2013; Viviroli and Weingartner, 2004; Wu et al., 2015). The cryosphere (i.e. water in mountainous, alpine regions stored as glaciers, snow, permafrost, and rain) plays a critical role in moderating water availability to downstream watersheds (Gao et al., 2018). It temporally

https://doi.org/10.5194/hess-2022-160
Preprint. Discussion started: 2 May 2022

redistributes winter precipitation to higher demand periods like the spring and summer (Viviroli et al., 2011) and reduces the variability of flow (Wang and Cheng, 2000).

High latitude, cold regions have greater sensitivity to global warming (Chen et al., 2018; Jones and Rinehart, 2010; Zhang et al., 2020). The warming rate in the Tibetan Plateau, the largest and highest mountain-range in the world, is twice the global rate (You et al., 2020). This accelerated warming of the cryosphere has substantially altered water cycles and streamflow (Chen et al., 2018; Wu et al., 2015; Xu et al., 2015; Zhang et al., 2016). Alterations in the quantity of cryosphere water storage and timing of discharge can change downstream water availability and human water allocations (Chen et al., 2018; Xu et al., 2015). However, the impact of cryosphere melting on downstream systems is not fully understood.

The Heihe River Basin is an example of a system that has been impacted by the warming climate. It is a semi-arid, agriculturally important region located in Northwestern China (Figure 1). The Qilian Mountain cryosphere in the upper basin is the region's primary water source (Wang and Cheng, 2000; Zongxing et al., 2016). The movement of water from the high precipitation upper reaches to the arid valley floor has been critical for downstream development (Liu et al., 2019a). It has allowed for the expansion of irrigated agriculture which accounts for over 90% of water usage in the middle basin (Chen et al., 2005; Deng and Zhao, 2015; Sun et al., 2016). However, this reliance on water from the upper reaches makes the middle basin vulnerable to warming induced changes in the cryosphere than other areas with higher local precipitation (Kang et al., 1999).

The upper basin is expected to undergo significant changes in glacier volume, permafrost coverage and precipitation due to climate change. Future projections for Northern Asia, where the Heihe River Basin is located, indicate precipitation will likely increase (Shi et al., 2006; Zhang et al., 2016). However, estimates for the timing and volume of future precipitation in high mountain areas are variable (IPCC, 2014). Increasing warming trends on the other hand are essentially certain (IPCC, 2014). Thus, in this study we focus on processes resulting from increased temperature alone, such as glacier and permafrost degradation.

Glacial contribution to streamflow is of particularly high importance in arid basins (Viviroli et al., 2011). Glaciers can stabilize flows, especially during hot or dry years (Chen et al., 2015; Qin et al., 2014). The ability of glaciers to buffer streamflow depends on glacial volume, melt rate, and the balance with evapotranspiration. Under climate warming, it is estimated that glaciers in the upper basin may disappear entirely by the middle of the century (Chen et al., 2018; Wu et al., 2015). In this case, the glacial contribution to flow, and its moderating effect in warmer months will eventually vanish.

Warming temperatures have also caused significant permafrost degradation in alpine regions around the world, including the Qilian Mountain cryosphere (Gao et al., 2018; Ma et al., 2019; Niu et al., 2010; Song et al., 2019). Permafrost acts as an impermeable boundary to infiltrating water. For this reason, permafrost dominated catchments tend to have higher peak, and lower base flows, with primarily short, lateral groundwater flow paths (Carey and Woo, 2001; Niu et al., 2010; Ye et al., 2009). When permafrost degrades, hydraulic conductivity increases and water can infiltrate to deeper depths and take longer flow paths (Ma et al., 2019; Niu et al., 2010). This results in lower peak flows, as more water infiltrates instead of running off, and higher base flows as more groundwater enters streams (Carey and Woo, 2001; Ma et al., 2019). There is also

https://doi.org/10.5194/hess-2022-160
Preprint. Discussion started: 2 May 2022

an increase in the volume of ground-ice meltwater, which is the release of water stored as ice within permafrost (Ma et al., 2019).

Many studies have examined the contribution of glacial melt water to streamflow in the upper Heihe River Basin. These estimates range from 3%, up to about 10% for the Heihe River (Chen et al., 2018; Chen et al., 2015; Gao et al., 2018; Niu et al., 2010; Wu et al., 2015; Zongxing et al., 2016). The contribution to smaller rivers, like the Hulugou, may have a meltwater contribution as high as 32% (Zongxing et al., 2016). This contribution only occurs during the thawing season, which is from April to October (Gao et al., 2018). There is not full agreement on how much these glaciers contribute to total flow, and what streamflow may look like after they disappear.

Previous work has also quantified the impact of permafrost degradation on streamflow. Increasing winter streamflow trends in alpine regions can be attributed to permafrost degradation processes as there are very few alternate sources of water at this time (Gao et al., 2018; Ma et al., 2019; Niu et al., 2010). This increase is often only significant in basins with initially high permafrost coverage (Niu et al., 2010; Ye et al., 2009) such as the Heihe River Basin. The estimated increase in runoff in the freezing season from permafrost degradation in the upper Heihe River Basin is around 50% from 1971 to 2010, associated with an 8.8% loss in permafrost area (Gao et al., 2018). While the change in flow is measured during the freezing season, degrading permafrost could impact baseflow in all seasons (Jones and Rinehart, 2010; Walvoord and Striegl, 2007).

Numerical, process-based hydrologic models have been used to study the Heihe River Basin. Cryosphere response to global warming in the upper basin was studied by Chen et al. (2018) and Gao et al., (2018). Models have also been used to examine a wide range of water resource issues in the middle and lower reaches of the Heihe River Basin. For example, the ecohydrological model HEIFLOW has been used to simulate groundwater-surface water interactions, agricultural operations, ecohydrological response, and reservoir impacts amongst other topics (Han et al., 2021; Sun et al., 2018; Tian et al., 2018; Tian et al., 2015a; Tian et al., 2015b; Yao et al., 2018; Yao et al., 2015a; Yao et al., 2015b). However, to our knowledge, no studies have examined the impact of changes in upper basin streamflow due to cryosphere processes on both ground and surface water in the middle basin.

We address this gap by modeling the middle basin response to cryosphere changes using the integrated hydrologic model ParFlow-CLM. ParFlow-CLM is designed to capture dynamically evolving interactions between groundwater, surface water and land surface fluxes (Jones and Woodward, 2001; Kollet and Maxwell, 2006; Kollet and Maxwell, 2006; Maxwell et al., 2015). It is thus, well suited to examine evolving watershed dynamics. Using this approach we explore how groundwater-surface water interactions and water storage in the middle basin evolve as a result of changing streamflow coming from the cryosphere, how these processes vary seasonally, and how projected warming in the middle basin can shift this response.

https://doi.org/10.5194/hess-2022-160
Preprint. Discussion started: 2 May 2022

Hydrology and Earth System Sciences
Open Access
Discussions

2 Data and Methodology

2.1 The Study Area

The Heihe River Basin is a semi-arid catchment with an area of approximately 130,000km^2 in Northwestern China (Figure 1). It is located in the Hexi corridor, one of the most arid regions in the world (Lu et al., 2015). The basin decreases in elevation and increases in temperature and aridity moving from south to north. Elevation varies from about 5600 to 900m (Yao et al., 2018), long-term average temperature ranges from -4C to 10C (Liu et al., 2019a), precipitation from 800mm to below 50mm (Liu et al., 2019a) and PET from 700mm (Zhang et al., 2015b) up to 2300mm (Deng and Zhao, 2015).

The Heihe basin has three principal sections: the Upper, Middle and Lower basin. The Upper basin is located at the Northern edge of the Tibetan Plateau and contains the Qilian mountains and the headwaters of the Heihe River, the largest river in the basin. This is the primary runoff generation area for the rest of the basin, contributing about 70% of total river runoff in the lower reaches (Liu et al., 2019; Yang et al., 2014). The middle Heihe is a flat oasis area where most human settlement and economic activity is located. The middle basin uses an estimated 80-95% of the available fresh water from the entire system (Deng and Zhao, 2015; Liu et al., 2009; Sun et al., 2016; Yang et al., 2015; Yao et al., 2015b). Of this, 80-90% of it is consumed by irrigated agriculture (Chen et al., 2005). The Lower basin is primarily Gobi Desert and has little human development. It contains the two terminal lakes of the Heihe River.

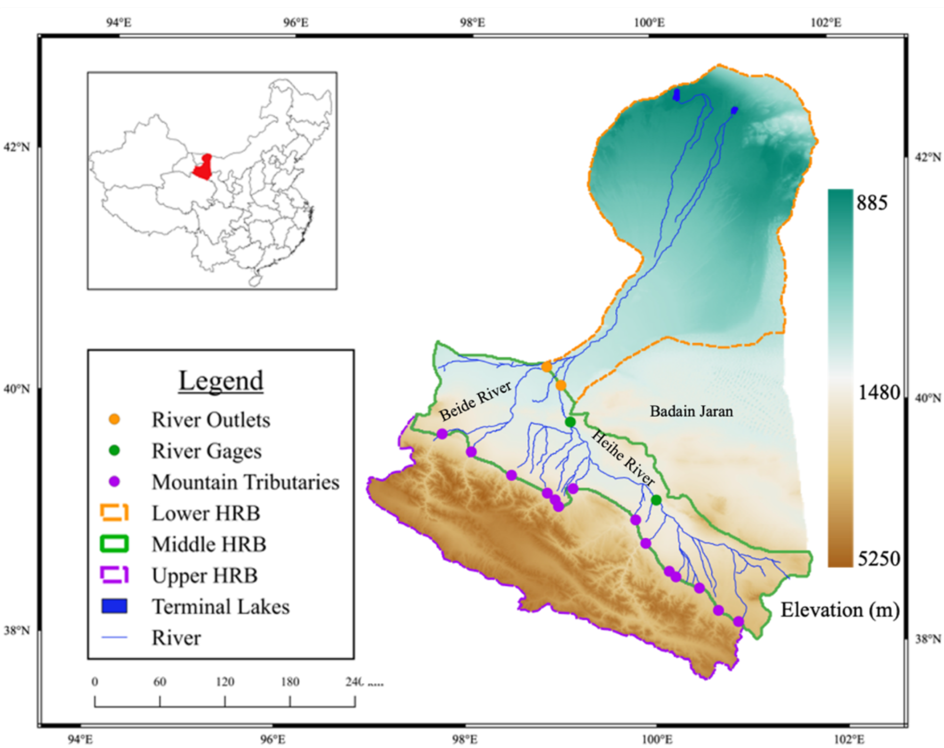

https://doi.org/10.5194/hess-2022-160
Preprint. Discussion started: 2 May 2022

Hydrology and Earth System Sciences
Discussions

Figure 1: Location of the Heihe River Basin in China shown in red in the inset. The upper basin is outlined in purple, the middle basin in green and the lower basin in orange. The Badain Jaran Desert is labelled and is hydrologically connected to the basin. The gaged inflow locations between the upper and middle basin are in purple. The two river gages on the main stem of the Heihe river are in green and were used for calibration. The location of the Beide and Heihe river outlets are shown in orange. The two terminal lakes are colored in blue at the end the river network. Elevation ranges from about 5250m to 885m and is shown in the legend to the right.

2.2 Hydrologic Modeling Approach

We elected to use the integrated hydrologic model ParFlow-CLM in this study. ParFlow-CLM is an integrated hydrologic modeling platform that simulates both surface and subsurface processes together. It has been used extensively in hydrologic studies of groundwater-surface water interactions, the food-energy-water nexus and climate change in small to large sized basins, including the entire continental US (Condon et al., 2020; Condon and Maxwell, 2014; Ferguson and Maxwell, 2010; Hein et al., 2019). ParFlow-CLM has also been used to model the Central Valley in California, a semi-arid, mountain-valley agriculture system with many parallels to the Heihe River Basin (Gilbert and Maxwell, 2017, 2018; Thatch et al., 2020). In the subsurface, variably saturated flow is solved using the mixed form of Richards Equation. Overland flow is solved by the kinematic wave approximation and Manning's equation. Further details about the workings of ParFlow are provided in: Ashby and Falgout, 1996; Jones and Woodward, 2001; Kollet and Maxwell, 2006; Maxwell et al., 2015; and Maxwell, 2013). ParFlow is coupled to the Common Land Model (CLM). CLM is a land surface model which handles the surface water-energy balance (Maxwell and Miller, 2005; Kollet and Maxwell, 2008).

There has been previous hydrologic model development in the Heihe basin. HEIFLOW is a GSFLOW (Coupled Ground-Water and Surface-Water Flow Model) based model (Markstrom et al., 2008). GSFLOW was developed by the USGS and couples MODFLOW (Modular Ground-Water Flow Model) and PRMS (Precipitation-Runoff Modeling System). The vadose zone, rivers, lakes and other components are defined ahead of time and handled by coupled packages. GSFLOW was enhanced across several studies to include modules which handle surface diversion and pumping (Tian et al., 2018; Tian et al., 2015a; Tian et al., 2015b), dynamic vegetation growth (Sun et al., 2018) and sub grid parameterization of soil and irrigation water (Han et al., 2021).

The primary difference between the ParFlow-CLM model we present here and HEIFLOW is that ParFlow solves variably saturated flow in all subsurface cells. Additionally, overland flow is fully integrated with the subsurface in ParFlow through a free surface overland flow boundary condition that allows rivers to form and disappear as moisture changes. The approach used by ParFlow means that there is no need for a-priori specification of saturated zone, vadose zone, river network, etc. prior to simulation. This approach allows for a dynamic evaluation of groundwater-surface water interactions. This capability is of importance in modeling the Middle Heihe because of the high rate of conversion between surface and groundwater (Yao et al., 2015a; Wang and Cheng, 2000).

https://doi.org/10.5194/hess-2022-160
Preprint. Discussion started: 2 May 2022

2.3 Model Inputs

Unless otherwise stated, the data used in the model were originally obtained from the Heihe Program Data Management Center (HPDMC) (http://www.heihedata.org). If data was altered from the original form from the HPDMC, the publication which details that alteration is given as opposed to the original data repository in Table 1. For example, some of the data underwent pre-processing and parametrization to be used in the construction of the HEIFLOW model for which details can be found in (Tian et al., 2018; Tian et al., 2015a; Tian et al., 2015b). This data served as our source data and will be referred to as such throughout the paper.

Table 1. Source Data

Starting Variable	Data Soure	Original Units	Spatial Resolution	Time of Data	Model Input
Geolayers	Yao et al., 2014	m	1kmx1km	2000	Vertical Discretization
DEM	HPDMC	m	1kmx1km	2008	X/Y Slopes
Hydraulic Conductivity (K)	Tian et al., 2015	m/day	1kmx1km	2000	K
Specific Storage (SS)	Tian et al., 2015	1/m	1kmx1km	2000	SS
Specific Yield (SY)	Tian et al., 2015	[]	1kmx1km	2000	Porosity (n)
Groundwater Boundary Condition (GWBC)	Tian et al., 2015	m3/day	Boundary grids	average from 2000-2012 Annual Data	GWBC
Surface Water Boundary Condition (SWBC)	HPDMC	m3/s	14 Stations	2000-2012 (daily/monthly)	SWBC
Landcover	HPDMC	NLUD-C	1kmx1km	2011	Landcover, Mannings values

ParFlow-CLM requires gridded inputs for hydraulic conductivity (K), specific storage and porosity. The source data for K was parameterized in Tian et al. (2015a) resulting in 92 unique values ranging from 0.001 to 5.625 m/h. We aggregated these values for our study into 15 soil and 15 geological units to facilitate adjusting by hydrogeologic group in our calibration process. We also assigned a value of 0.001 m/h to regions in the vertical domain of the PF-CLM model that had no source data. The intention is for this region to be considered bedrock.

The source data had information regarding specific yield but not the required variable, porosity. As mentioned previously, most of the domain acts as an unconfined aquifer, with only locally confining conditions (Yao et al., 2015a; Yao et al., 2015b) which are not obvious at our spatial resolution. For this reason, specific yield was used as an analog for porosity. We also simplified the values in the specific yield data from 17 unique values ranging from 0.05-0.35 as calibrated in Tian et al. (2015a) to three intervals of 0.1, 0.2 and 0.3 to lessen computational demand.

Specific storage had two unique values and was assigned by hydrogeologic unit. We categorized the porosity and specific storage variables into seven groups, six for each unique pair of porosity and specific storage values and a seventh group representing bedrock for regions in our vertical domain that have no source data. This group was assigned the lowest value from the source data for each respective variable. This corresponds to 0.05 for porosity and $1.0^{-4}m^{-1}$ for specific storage. These values are corroborated by the literature as reasonable values for bedrock (Huntington and Niswonger, 2012).

Hydrology and Earth System Sciences
Open Access
EGU
Discussions

The raw Digital Elevation Model (Table 1) was processed to ensure adequate surface drainage of every cell in the domain to either the stream network or domain boundary. The process was accomplished using PriorityFlow, an open-source R package which is a modified priority flood and global slope enforcement algorithm (Condon and Maxwell, 2019). The result is a smoothed, fully draining DEM which was used to produce X and Y slope files which are the required input for PF-CLM. The processed DEM was also used to calculate drainage areas and stream orders which were later used to define the Manning's roughness parameters.

The land cover dataset used is the NLUD-C (National Land Use / Cover Database of China) for 2011 (Table 1). Land cover has not been static over the period of simulation. For example, farmland, forest and built-up land have all increased due to the expansion of agriculture and other economic activity in the basin while grasslands, water bodies, wetlands and desert have all decreased, likely converted to the previous land types (Hu et al., 2015). However, land conversion slowed considerably after the year 2000, and most natural oases in the basin had already been converted to farmland by 1975 (Lu et al., 2015). In addition, future land-use patterns are not expected to be appreciably different from the year 2000 (Zhang et al., 2015b). For these reasons, we made the decision to use the 2011 land cover map for our simulations. The land cover map was converted from NLUD-C to IGBP (International Geosphere-Biosphere Programme) classification as that is the categorization required by CLM. NLUD-C categories were matched with the closest IGBP group based on descriptions. In some cases, CLM parameters such as LAI or canopy height were altered to better match with the NLUD-C land cover categories. The result is an 18 category IGBP land cover map that matches the 2011 NLUD-C map. Finally, the IGBP land cover map and the stream order map of the domain produced by the topographic processing workflow were used to create a spatially variable Mannings roughness value grid. The conversions for land type and stream order to Mannings value were obtained from Foster and Maxwell (2018) and the 2015 WRF Hydro User Guide version 3.0 (Gochis et al., 2015).

The climate forcing variables required to run CLM are long and shortwave radiation, precipitation, atmospheric pressure, specific humidity and u and v wind components. The input climate dataset used is CMFD (China Meteorological Forcing Dataset) detailed in He et al. (2020). It has a temporal resolution of three hours and a spatial resolution of 0.1 degrees or about 10km. Although there are several other climate forcing datasets available, this one was selected as it had almost all the variables required to run CLM, was available for the entire simulation period, and has good spatial and temporal resolution. In order to fit the data to our 1km modeling grid, the climate data from CMFD was extracted and resampled. Then, the three-hour time step was divided to a one-hour time step where each span of three hours contains the same average data. The CMFD data only contained total wind as opposed to the u and v wind vectors required by CLM. To address this issue, we used wind direction data generated by a high-resolution regional climate model specifically designed for the Heihe River Basin (Xiong and Yan, 2013). This was used to derive the wind direction angle which was then applied to the CMFD wind magnitude to obtain u and v wind components.

https://doi.org/10.5194/hess-2022-160
Preprint. Discussion started: 2 May 2022

Hydrology and Earth System Sciences Discussions

2.4 Model Configuration and Initialization

The modeling domain selected is the Middle Heihe as shown in Figure 1 (green outline). The horizontal resolution of the model is 1-km with $nx = 360$ and $ny = 270$. This is the resolution of most of the source data (Table 1). The domain is divided into 14 vertical layers of varying thickness (note there is no lateral variation in thickness) as follows: 0.1, 0.3, 0.6, 1.0, 10.0, 10.0, 30.0, 30.0, 30.0, 30.0, 30.0, 100.0, 100.0 and 100.0 m. The top four layers correspond to soil and the bottom ten are geologic layers. This results in a total depth of 472m. The thickness of the bottom 10 layers was determined based on the 3D subsurface inputs for the HEIFLOW model of the basin. The HEIFLOW model had five vertical layers that vary in thickness laterally and correspond to the shallow unconfined aquifer, the first aquitard, the shallow confined aquifer, the second aquitard and the deep confined aquifer (Yao et al., 2015b). We designed our layers to best capture the spatial features of the HEIFLOW layering while maintaining constant thickness laterally.

We apply a constant flux boundary condition along the border between the Upper and Middle Heihe and no flow boundaries along the rest of the subsurface. The flux for the boundary with the upper basin was calculated using outputs from the HEIFLOW model which spans this boundary (Tian et al., 2015b; Tian et al., 2018) (Table 1). The components of subsurface flow entering below our model domain depth of 472m were subtracted. The remaining flux was applied evenly to all non-bedrock cells along the boundary (i.e. K greater than 0.004 m/h) (Gleeson et al., 2014; Huntington and Niswonger, 2012). This resulted in a flux value of $1.7^{-4} m/h$ applied to all non-bedrock cells on the southern boundary.

There are 14 gaged rivers entering the middle basin from the upper basin (Figure 1). We inject water into the model according to the flow at these gages. While many of the stream gauges have daily data, others only have monthly data (Table 1). In cases where daily data for a gage does not exist, the daily fraction of monthly flow was calculated for the closest gage with daily data. These fractions were then multiplied by monthly flow to interpolate daily data for the target stream gage. In our model, about 75% of water coming into the middle basin domain is from streamflow, 20% from precipitation, and 5% from the groundwater boundary condition.

Initialization of the ParFlow-CLM model was performed in two parts. First, steady-state equilibrium was achieved by running ParFlow on its own using a long-term recharge forcing at the land surface. The long-term recharge forcing was derived as the average difference between precipitation and evapotranspiration. The initialization began from a uniform water table 20m below the ground surface. It ran for 115 years and was determined to be complete when the storage change as a percent of recharge fell below 1%. Following this step, a two-year spin up using 2011WY climate forcings with PF-CLM was performed. The resulting pressure file was used as the starting point for all model calibration described below. After final parameters were selected, a new spin-up was performed which ran for 55 years with ParFlow only, and 18 years with PF-CLM using the 2001WY and 2002WY climate forcings. Once the percent difference in subsurface storage from year to year fell below one percent, initialization was judged to be complete.

https://doi.org/10.5194/hess-2022-160
Preprint. Discussion started: 2 May 2022

Hydrology and Earth System Sciences
Open Access
Discussions

For model calibration, streamflow observations from the 2011WY at two gages, HRB1 and HRB2, as well as average water table depth (WTD) at 44 groundwater observations wells were used to assess model performance. Calibration was performed by manually adjusting the groundwater boundary condition, K and Mannings roughness coefficients.

2.5 Cryosphere Melt Scenarios

We designed five scenarios to model the middle basin response to future climate change. (1) A *Baseline* scenario, which uses historic climate and streamflow data to model the middle basin in a natural flow state. Next, three scenarios explore the Middle Heihe response to changing streamflow input from the cryosphere as a result of warming; (2) a *Glacier* scenario simulating the loss of the glacier contribution to streamflow after they are fully melted, (3) a *Permafrost* scenario capturing increases to baseflow as a result of permafrost degradation (4) a *Combined* scenario, which models both the glacier and permafrost changes to streamflow together. Finally, (5) a *Warming* scenario captures temperature increase in the Middle Basin.

The above scenarios are modeled for the simulation period of the 2001 Water Year (WY) to the 2011WY. This period was selected for three reasons. The first is data availability. The second is that we are interested in changes in groundwater storage. As groundwater is slow moving, if we want to capture the longer-term trends in storage, it is important to simulate for as many years as possible. Last, the period is representative of wet, normal and dry years which makes it ideal to examine climate impacts on hydrologic processes (Tian et al., 2018).

The *Baseline* scenario represents observed historical conditions. Here we apply daily streamflow from historic data at the 14 gage locations between the upper and middle basins (Figure 1). Figure 2 shows idealized annual streamflow separated into components. For the *Baseline*, all three components are applied at their historic fraction throughout the year. The light-blue, precipitation component, which consists of rain and snowmelt, remains unaltered in all scenarios.

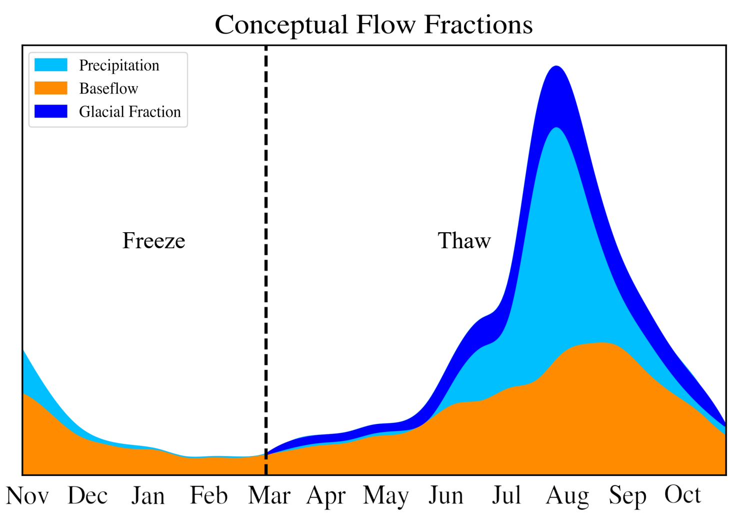

https://doi.org/10.5194/hess-2022-160
Preprint. Discussion started: 2 May 2022

Hydrology and Earth System Sciences
Discussions

Figure 2: Conceptual model of streamflow with each of the flow components highlighted. Freeze and Thaw refer to times of year where we expect water to melt in the cryosphere (thaw) or remain frozen (freeze). The precipitation fraction is light blue and consists of rain and snowmelt. This fraction is unaltered in the scenarios. The glacier fraction is dark blue. This fraction corresponds to 15% in the scenarios and is removed from streamflow during the thawing season for Glacier, Combined and Warming. The orange fraction represents baseflow and is increased by 50% in the Permafrost and Combined scenarios.

The *Glacier* scenario is designed to represent a future in which the glaciers in the upper basin have completely disappeared. To do this we remove the fraction of streamflow contributed by glacial melt during the thawing season (April to October). This is represented by the dark blue component in Figure 2. Freezing and thawing periods were taken from (Gao et al., 2018). The current contribution of glacial melt to upper basin streamflow is uncertain but has been estimated by several studies focusing on the impact of glacial melt on streamflow in the upper basin (Chen, 2014; Chen et al., 2018; Gao et al., 2018; He et al., 2008; Wu et al., 2015; Yang, 1991; Zongxing et al., 2016). Based on these studies we chose to subtract 15% from total streamflow. We purposefully chose a percentage on the upper end of those estimated in the literature to see if there is any impact from the maximum possible reasonable flow reduction.

The *Permafrost* scenario models changes in streamflow as a result of permafrost degradation. The baseflow component of streamflow, shown in orange in Figure 2 (orange shading) is altered in this scenario. Gao et al. (2018) found that winter runoff has increased about 50% from 1970 to 2010 corresponding to an 8.8% reduction in permafrost area. Assuming a similar, or greater loss of permafrost area in the future, we chose to increase our baseflow by 50% for the *Permafrost* scenario. We apply this increase year-round as opposed to only in the freezing or thawing season because subsurface permeability changes and enlargement of the groundwater reservoir due to permafrost degradation would impact streamflow all year.

To apply the baseflow change, we performed baseflow separation on the observed streamflow using the digital filtering method outlined in Liu et al. (2019b). Digital filtering separates high- from low-frequency signals, in this case runoff from baseflow. Equation (1) solves for surface runoff at the current time step (Q_{dt}) and Equation (2) solves for baseflow (Q_{bt}). β is the filtering parameter and T is the number of passes with the digital filter. The initial parameterization for β and T was taken from estimates for the Upper Heihe basin (Liu et al., 2019b; Zhao et al., 2016) as 0.95 and three respectively. After visual inspection, β = 0.90 and T = 3 were selected as the best fit for our data.

$$Q_{dt} = \beta Q_{d(t-1)} + \frac{(1+\beta)}{2}\left[Q_t - Q_{(t-1)}\right] \quad (1)$$

$$Q_{bt} = Q_t - Q_{dt} \quad (2)$$

The *Combined* scenario represents a system where changes in flow due to glacial melt and permafrost degradation are occurring at the same time. For this case we apply perturbations to streamflow that are identical in timing and volume to those made in both the *Glacier* and *Permafrost* scenarios (i.e. 15% reduction in thawing season flow and 50% reduction in

https://doi.org/10.5194/hess-2022-160
Preprint. Discussion started: 2 May 2022

Hydrology and Earth System Sciences
Discussions

baseflow year round). In many ways the *Combined* scenario is the most realistic future representation of streamflow, as we do expect glacial reductions and permafrost degradation to both occur. We perform the isolated glacial and permafrost cases in order to quantitatively isolate the different signatures that these changes have.

The *Warming* scenario is designed to evaluate the impact of future warming in the middle basin on the hydrologic system. The *Warming* scenario is identical to the *Combined* scenario except for a global increase of 2C in the CMFD temperature forcing data. We selected 2C as it is a reasonable mid-century estimate for global temperature increase (IPCC, 2014). In line with previous studies, we decided that simplifying the temperature increase would allow us to better isolate the hydrologic response to warming (Condon et al., 2020).

3 Results

Results are organized into four subsections. Section 3.1 outlines the performance of the model with regards to streamflow and water table depth (WTD) observations. Section 3.2 covers all results related to streamflow specifically. This includes overall time series, anomalies from *Baseline* and seasonal patterns. Similar results are included in Section 3.3 for subsurface storage. Section 3.4 contains spatial results which allow for the assessment of warming impact in the scenarios.

3.1 Baseline Model Performance

To assess model performance, we compared model streamflow to observed data at gage HRB2 on the Heihe River. HRB2 is the furthest downstream gage and the closest to the outlet (Figure 1). The streamflow performance of the Baseline scenario is shown in Figure 3. It is important to note that we are modeling a natural flow state while the observational data is subject to operations like pumping and diversion. As we do not include these processes, we expect our model streamflow to be higher. For this reason, our main targets were to match winter baseflow (when there is little diversion) and streamflow timing.

We also apply diversion adjustments to observed streamflow to provide a more direct comparison to our natural flow state model. In order to approximate naturalized flows, we assumed that flow lost between an upstream and downstream gage roughly corresponds to the water diverted between stations (Zhang et al., 2015a). So, we quantified the flow lost between the inlet and the HRB1 gage, as well as between the HRB1 and HRB2 gage, and added that back to the streamflow time series for HRB2.

The difference between the observed and naturalized streamflow is illustrated in Figure 3b & c. Figure 3b shows the model (blue) and observed (red) in 2001 with no correction applied. The model matches baseflow in the winter months (November to February) as expected due to minimal diversion. However, in warmer months when water begins to be diverted and pumped for irrigated agriculture, observed flows drop to essentially zero, while the simulated flow remains high. Figure 3c shows the same year comparing the naturalized streamflow with simulation. As expected, there is little change in the winter months. However, in the warmer months, we match the magnitude of flows more closely.

https://doi.org/10.5194/hess-2022-160
Preprint. Discussion started: 2 May 2022

Figure 3a shows the model comparison to the naturalized streamflow data for the entire period of simulation. We used Spearman's rho as a metric to determine correlation. It tests that the model is increasing or decreasing at the same time as the observed data. This helps quantify how well we match streamflow timing. The Spearman's rho is 0.72 showing a good positive correlation. However, the model flow still tends to overestimate the peak flows. This is likely due to remaining bias in the model as well as the simplicity of our flow correction. The naturalized flow correction is not perfect, and doesn't account for the impacts of groundwater pumping, or diversion on other tributaries draining into the Heihe River.

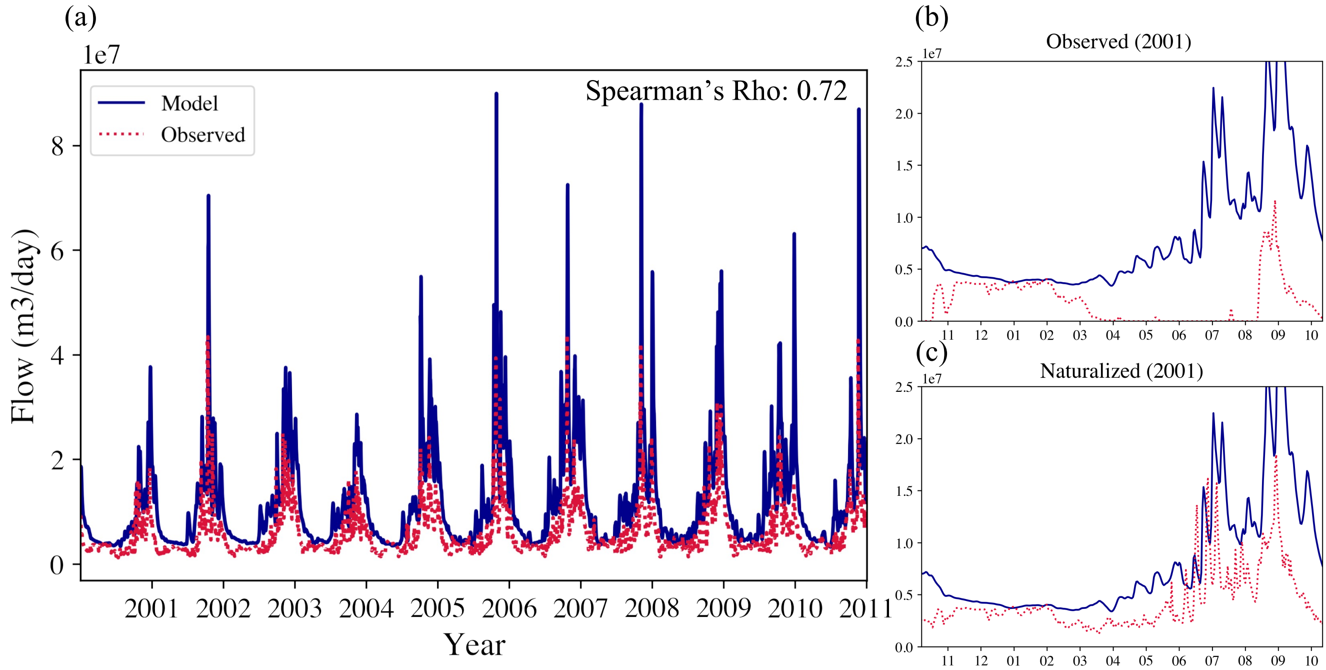

Figure 3: A comparison of observed and model flow at the HRB2 gage. (a) shows the model flow in blue for the entire simulation period compared to naturalized flow data for HRB2. (b) shows the original observed data in red, which was not subject to consumption correction for the year 2001. Each number refers to a month, and November to October is shown. (c) shows the same year but with the naturalized flows in red. Spearman's rho was calculated for the comparison to naturalized flows.

The *Baseline* performance for WTD at 44 observation wells is shown in Figure 4. The model WTD generally falls within 10m or less of the observation wells. However, the simulated WTD is significantly shallower where the Heihe River crosses the boundary between the upper and middle basin. This is illustrated by the three dark green dots (Figure 4). This is an area of high K (around 5.6m/hour) and as a result, without the pumping and diversion that occur here in the managed system, a much greater volume of water can infiltrate at a rapid rate compared to other parts of the domain and raise the model WTD.

https://doi.org/10.5194/hess-2022-160
Preprint. Discussion started: 2 May 2022

Hydrology and Earth System Sciences
Open Access
Discussions

There are three additional outlier points where the model WTD is much deeper than expected (orange). The discrepancy at these points is likely to do with our spatial resolution and uncertainty of the actual well locations in our domain. These wells all occur in locations where there is a sharp gradient in WTD due to elevation changes from a mountain range in the North. These three observation wells are located in this steep area where water table depths are very sensitive to location. Overall, based on the results of both streamflow and WTD, we conclude that the model performs satisfactorily when the natural flow state is considered.

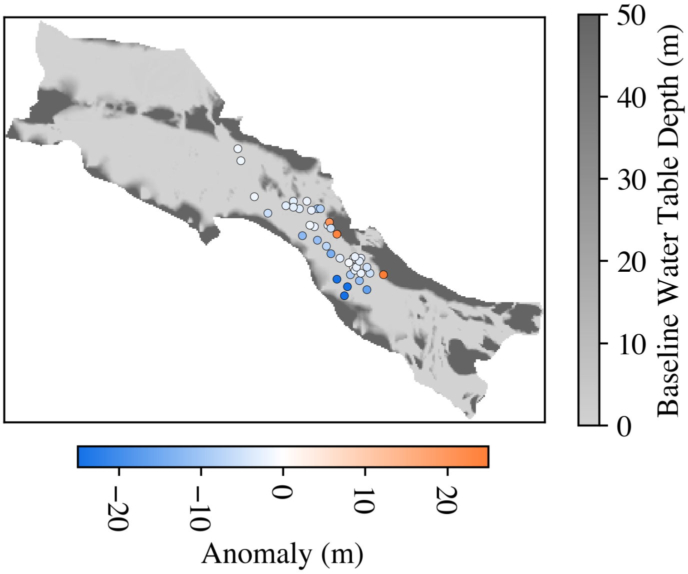

Figure 4: The points refer to the locations of the 44 observation wells in the middle basin. They are colored by the difference of the average observed water table depth and model water table depth for the *Baseline* simulation across the simulation period (2001WY to 2011WY). A negative value (green) means the model has a shallower water table, while a positive value (orange) means the model has a deeper water table than observed. A value of zero (white) means there is no difference. The background (gray) shows the mean *Baseline* water table depth for the simulation.

3.2 Streamflow

A streamflow time series at the outlet of the Heihe River for each of the five scenarios is shown in Figure 5. Flows are low in the colder months, consisting almost entirely of baseflow. Most of the streamflow occurs in the late summer and early fall, with high and peaky flows. There is strong overlap between the scenarios, showing that all our climate warming cases still result in consistent overall behavior during simulation. When scenarios do diverge from *Baseline*, it is typically in the expected order. The *Permafrost* scenario (green), has the highest net increase in flow, followed by the *Combined* (yellow) and *Warming*

https://doi.org/10.5194/hess-2022-160
Preprint. Discussion started: 2 May 2022

(orange) scenarios. The *Glacier* scenario (blue) is the only one with flow below the *Baseline*, except for very occasionally, *Warming*.

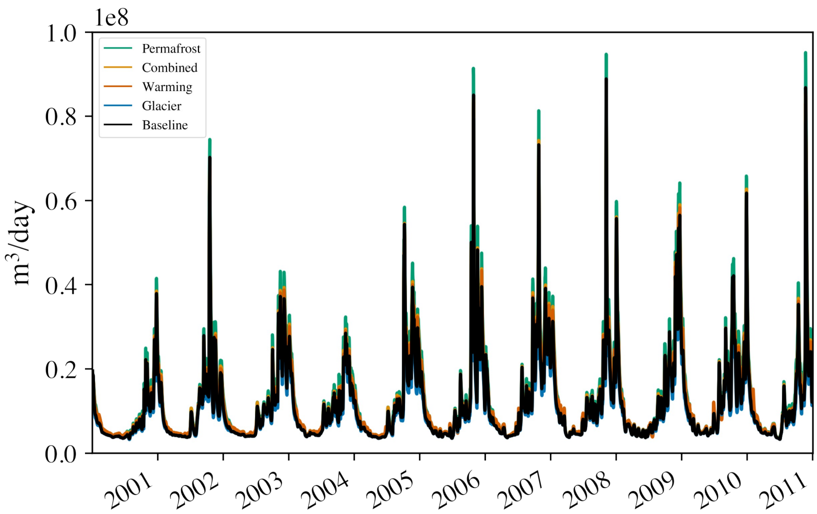

Figure 5: Daily streamflow at the Heihe River outlet. Summed from hourly model outputs for the five scenarios: Baseline, Glacier, Permafrost, Combined and Warming. The scenarios were run from the 2001-2011WY.

To isolate the impacts we are observing in our scenarios from the baseline dynamics in the model, we primarily discuss our results in terms of how the scenarios differ from the *Baseline* scenario. Inflow perturbation refers to the difference in streamflow input between the scenarios and the *Baseline*. The outlet anomaly refers to the difference in flow at a river outlet. Storage anomaly refers to the difference in storage at a given time. The anomaly fraction (for outlet or storage) refers to the outlet or storage anomaly divided by the inflow perturbation.

Figures 6a and b show the inflow perturbation and outlet anomaly plotted together for the Heihe and Beide rivers. First, in Figure 6a for the Heihe river, we see that the outlet anomaly is always smaller in magnitude than the inflow perturbation. This means that as water moves from the inlet to the outlet, the inflow perturbation signal is dampened. That is, a negative inflow perturbation (reduction in water from *Baseline* flow) such as the *Glacier* scenario will become less negative. A positive inflow perturbation (increase in water input from *Baseline*), like the other three scenarios, will become less positive. The only exception is 2011 where the outlet anomaly is slightly less than the inflow perturbation for the *Permafrost* scenario.

In Figure 6b for the Beide river, we see this same dampening signal from 2001 to 2004 for the *Permafrost* and *Combined* scenarios and until 2005 for the *Glacier* scenario. After this year, the inflow perturbation starts to be amplified as opposed to dampened. This is represented in the figure by the outlet anomaly plotting below the inflow perturbation in the *Glacier* scenario, and above in the *Permafrost* and *Combined* scenarios. The *Warming* scenario however continues to exhibit dampening of the inflow perturbation throughout the simulation.

https://doi.org/10.5194/hess-2022-160
Preprint. Discussion started: 2 May 2022

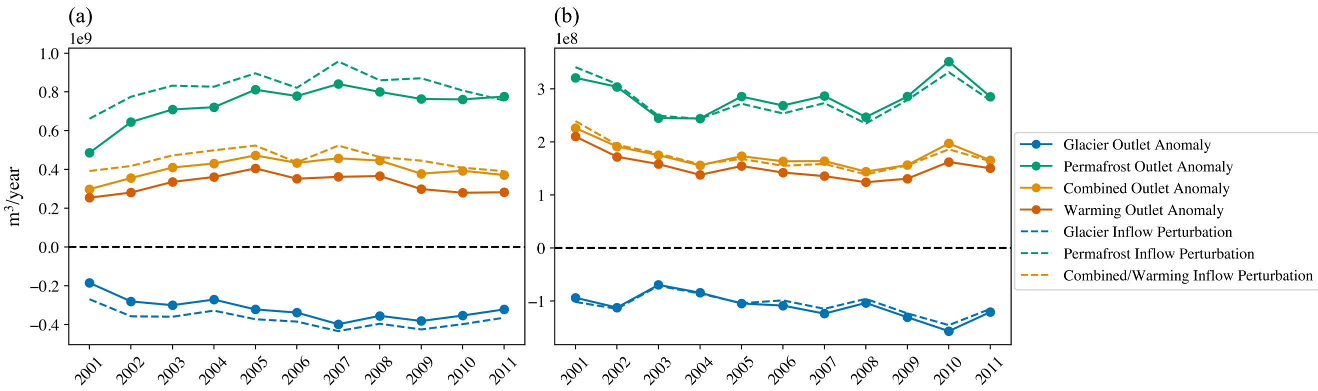

Figure 6: Inflow perturbations are shown in dashed lines, representing the magnitude of flow difference between the four scenarios and the Baseline. Solid lines show outlet anomalies, or differences between scenarios and Baseline at the outlet. (a) shows these two metrics for the Heihe River outlet while (b) shows the same for the Beide river outlet. The Heihe River is the drainage area for 12 tributaries, while the Beide River is the drainage area for two.

The anomaly fraction refers to the fraction of the inflow perturbation that is still present at the outlet, whether an increase or reduction (Figure 7). A fraction of one means that the anomaly at the outlet is equal to the inflow perturbation. A number less than one indicates that the outlet anomaly is less than the inflow perturbation and that the signal was dampened. A number greater than one indicates the outlet anomaly is more than the inflow perturbation or that the signal was amplified as it moved downstream. If a fraction is negative, it means that the outlet anomaly is the opposite sign of the inflow perturbation, that is a reduction in flow at the inlet becomes an increase in flow at the outlet or vice versa.

First in 7a, we see that the fraction is always less than one in all years, and all scenarios for the Heihe River, except in 2011 for *Permafrost*. This corroborates what we see in Figure 6a which is that the inflow perturbation is almost always dampened in the Heihe river drainage. The first year of simulation shows a large increase in fraction for all scenarios, with a smaller increase for the *Warming* scenario. After this point, there is an increasing trend in fraction for all scenarios from 2001 to 2006. *Combined* and *Glacier* both exhibit a small decrease in fraction from 2003 to 2004. After 2006, trends become much more variable, except for in the *Glacier* scenario which shows smaller fractional changes from year to year. The *Warming* and *Combined* scenarios show very similar patterns because they have the same inflow perturbation. However, the *Warming* scenario is shifted downwards and maintains a smaller fraction throughout. Its behavior diverges from *Combined* in 2010 and 2011. The *Permafrost* scenario shows slightly less variability compared to the *Combined* and *Warming* scenarios. It also exhibits a switch to amplifying behavior in 2011.

The Beide River shows a large increase in anomaly fraction in the first year in all scenarios except *Warming*, which only has a small increase. This is similar to what is seen in the Heihe River. Likewise, there is a general increasing trend for *Glacier, Permafrost* and *Combined* scenarios until 2006. However, after this year behavior between the two drainages differs.

https://doi.org/10.5194/hess-2022-160
Preprint. Discussion started: 2 May 2022

Hydrology and Earth System Sciences
Discussions

There is a large jump in fraction for the *Glacier* scenario showing a switch to an amplification of the negative inflow signal. *Permafrost* and *Combined* also exhibit a switch to amplifying behavior and the fractions are not as variable as for the Heihe River. The differences between the *Warming* and *Combined* scenarios are also more apparent in the Beide than Heihe. The *Warming* scenario is clearly more variable than *Combined* in the Beide, however they are both similarly variable in the Heihe.

It should be noted that the range of the fractional changes are smaller for the Beide than Heihe river. The fractions for the Beide range between 0.83 (0.92 without warming) and 1.1 while for the Heihe they range between 0.65 (0.68 without warming) and 1.1 across all years and scenarios. Thus, the overall change in anomaly fraction from the start to end of the simulation period is greater in the Heihe River.

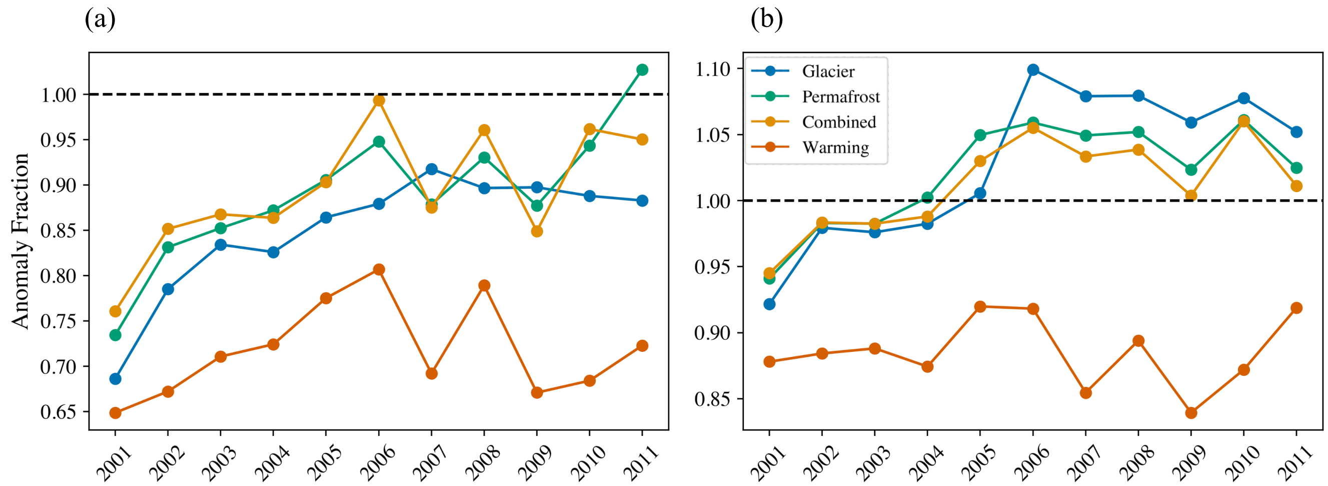

Figure 7: (a) shows the annual average anomaly fraction for the Heihe river and (b) for the Beide river for four scenarios (Glacier, Permafrost, Combined and Warming).

The anomaly fraction is also quantified on a monthly time scale to assess seasonal impacts (Figure 8). The anomaly fraction cannot be assessed for the *Glacier* scenario in the freezing season because the inflow perturbation is zero from November to March. The anomaly fraction generally increases for all scenarios across the thawing season (April to October) as total flows are increasing. However, the range of months over which the increasing trend persists varies. For *Glacier* and *Warming,* it begins in April. *Permafrost* has a few months delay, with the increase not beginning until June. The *Combined* scenario has the shortest and least consistent increasing window, from July to December. *Warming* and *Permafrost* also increase until December, whereas *Glacier* only increases until October, after which it cannot be assessed.

Variability tends to be consistent between most months across all scenarios. However, there are some months which stand out. These typically correspond to the periods with the lowest flows. For example, the inflow perturbation is closest to zero (black-dashed line) in April for *Glacier*, *Combined* and *Warming*. This month is clearly more variable for *Combined* and *Warming*, but not for *Glacier*. The *Permafrost* scenario has its smallest inflow perturbation in January, which also corresponds

https://doi.org/10.5194/hess-2022-160
Preprint. Discussion started: 2 May 2022

Hydrology and Earth System Sciences
Open Access
EGU
Discussions

to the month of greatest variability. However, the entire period of December to April has an inflow perturbation of similar magnitude, but notably different variability.

The anomaly fraction is always positive for *Glacier*, *Permafrost* and *Combined* in every month, however they do differ in the timing of dampening versus amplifying behavior (a fraction less than, as opposed to greater than, one). Looking at the mean anomaly fraction, the *Glacier* scenario only shows amplifying behavior in October. The *Permafrost* scenario has a mean anomaly fraction above one in November and December but shows significant amplifying behavior from September to January. The *Combined* scenario has strongly amplifying behavior in April, and the only other month where the mean fraction goes above one is December, with the rest of the year showing dampening. The *Warming* scenario is the only one to have a negative fraction at any time of year, with values often going negative in April and May. In these months, even though we added more flow than in the *Baseline* at the inlet, by the time the signal reaches the outlet, the flow is less than in the *Baseline*. Other than these months, *Warming* shows primarily dampening behavior outside of November, December and March.

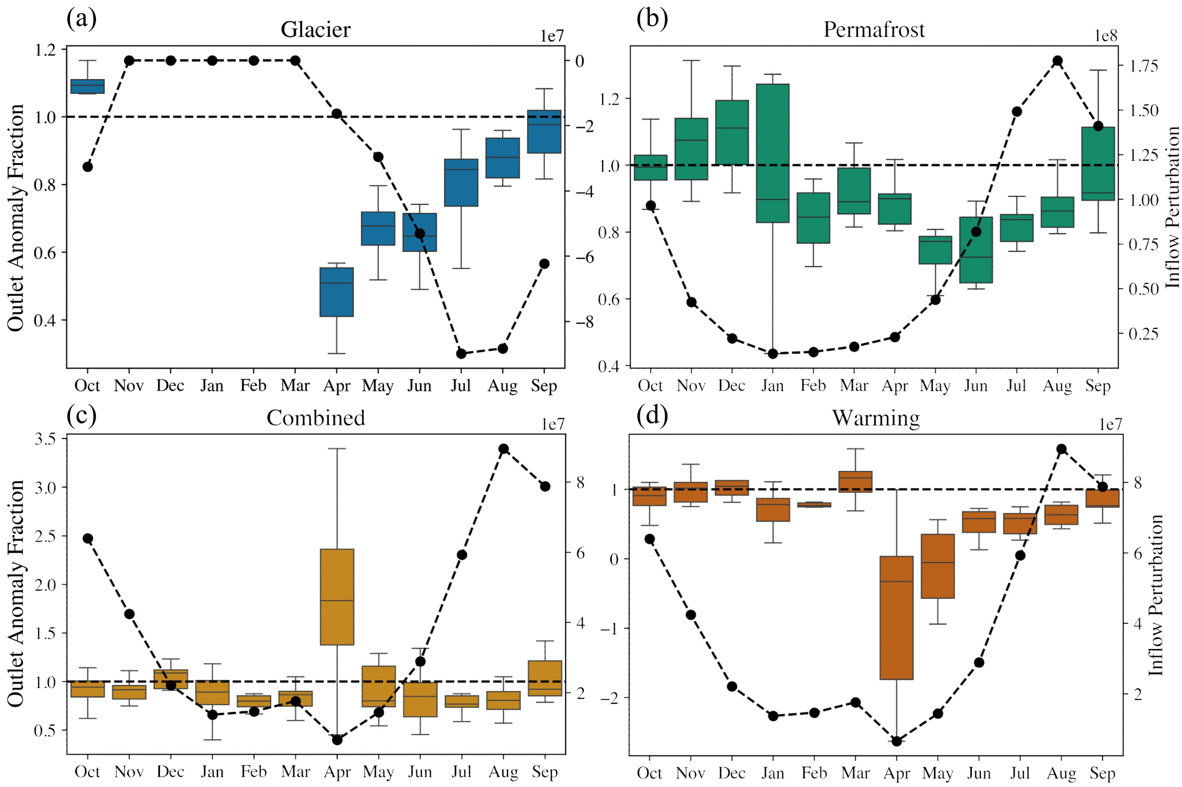

Figure 8: A boxplot of the monthly outlet anomaly fraction for the Heihe river outlet for each scenario is shown. (a) is the Glacier scenario, (b) Permafrost, (c) Combined and (d) Warming. The colored box represents the interquartile range (IQR) and the line in the center of it is the mean outlet anomaly in that month across all years of simulation.

https://doi.org/10.5194/hess-2022-160
Preprint. Discussion started: 2 May 2022

Hydrology and Earth System Sciences
Discussions

The whiskers extend from +/- 1.5IQR and cover 99.3% of the distribution. The outliers are not shown. Each point on the black dashed line is the average inflow perturbation in that month.

3.3 Subsurface Storage

Subsurface storage has a positive trend in all scenarios, including the *Baseline* (Figure 9a). Comparing storage trends relative to the *Baseline* we show that the largest increase in storage is *Permafrost* followed by *Combined* and *Warming*, with *Glacier* losing storage relative to *Baseline*. *Permafrost* and *Combined* have clear positive storage trends over the course of the simulation, except for 2011 for *Permafrost*. *Glacier* has a negative trend. The *Warming* scenario has a positive trend until 2005, after which it becomes more variable, with no clear trend.

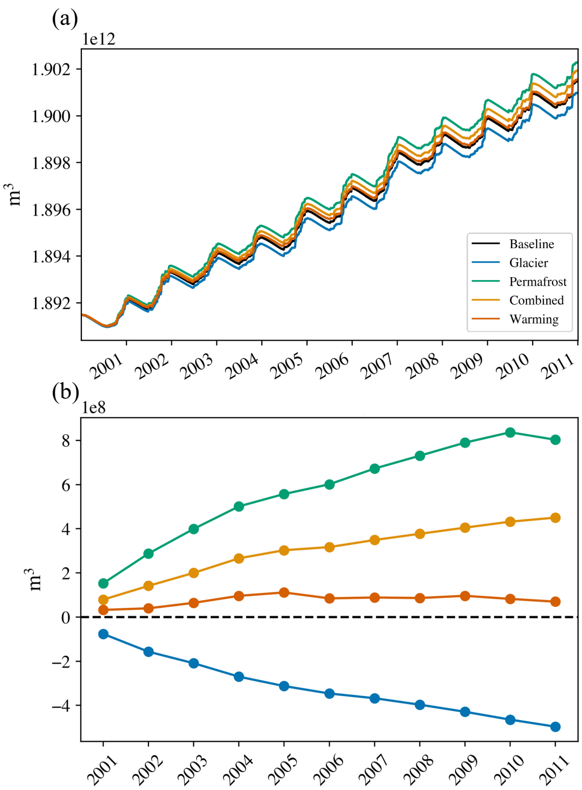

Figure 9: (a) timeseries of total daily subsurface storage for all scenario and (b) the anomaly of subsurface storage, calculated by removing Baseline storage from each of the scenarios.

The anomaly fraction for subsurface storage is shown in Figure 10 for (a) total storage (b) deep and (c) shallow (below and above 10m respectively). The *Glacier* scenario has exclusively negative fractions which indicates a net loss in storage relative to *Baseline*. The opposite is true for *Permafrost* and *Combined* which both have net gains in storage. In 2011, the negative fraction in the *Permafrost* scenario means that the *Permafrost* scenario did not gain as much storage as the *Baseline*

https://doi.org/10.5194/hess-2022-160
Preprint. Discussion started: 2 May 2022

Hydrology and Earth System Sciences
Discussions

in this year. The *Warming* scenario is variable from year to year, sometimes losing and sometimes gaining storage relative to *Baseline*.

All anomaly fractions in all simulations in the total (10a) and deep subsurface (10b) tend to approach zero. This decreasing trend is not as strong in the total subsurface (10a), which has a flatter trend. The shallow subsurface anomaly fraction (10c) is much more variable, where the fractions tend to approach zero until 2006, and then diverge again. The combination of deep and shallow subsurface trends likely causes the flattening we see in the total subsurface. A computed average of the anomaly fraction in the total subsurface after 2005 results in 0.06 for *Glacier*, 0.04 for *Permafrost* and 0.03 for *Combined* and -0.02 for *Warming*.

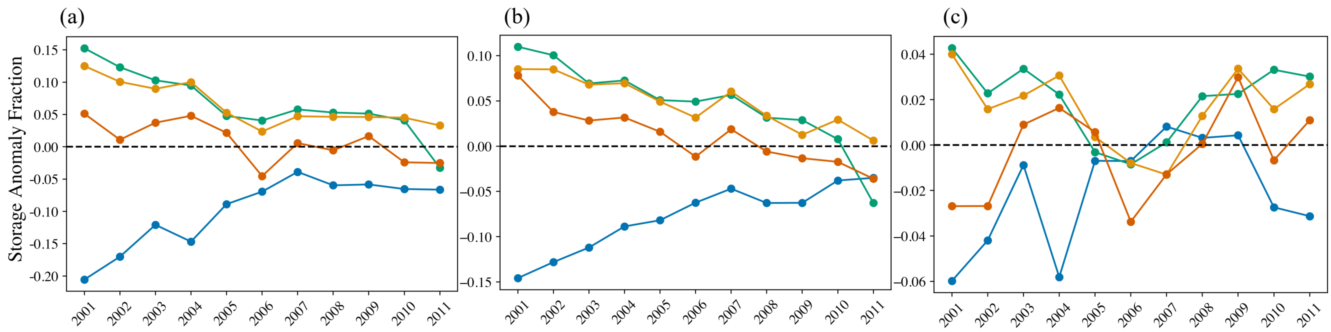

Figure 10: The subsurface storage anomaly fraction. (a) shows the time series for total subsurface storage while (b) is for deep subsurface storage, that is depths below 10m. (c) is shallow subsurface storage which corresponds to depths above 10m.

The mean anomaly fraction almost always shows dampening behavior (less than one) in figure 11. This indicates that a quantity of water less than the inflow perturbation applied is added or lost from groundwater storage. The only exception is the *Warming* scenario (11d) with positive amplifying behavior (fraction greater than one) in April and negative amplifying behavior (fraction less than negative one) in May. In April, this is interpreted as more flow than what was added at the inflow relative to *Baseline* being added to groundwater storage. In May, more water can be lost from groundwater storage than the inflow perturbation.

When the fraction is opposite the sign of the inflow perturbation, this represents changes in groundwater storage in the opposite direction as the inflow perturbation. In the *Glacier* scenario, this only occurs in April (11a). This means that in April, even though there has been a flow decrease, the monthly storage increase is greater than the *Baseline*. As for *Permafrost* (11b), while the mean fraction is never negative, there are months across the simulation period that are negative. This means that even though there is a relative flow increase, there has been a smaller increase in groundwater storage than *Baseline* that month. The *Combined* (11c) and *Warming* (11d) scenario both have months where the mean anomaly fraction is negative, May and June for *Combined* and May through August for *Warming*.

https://doi.org/10.5194/hess-2022-160
Preprint. Discussion started: 2 May 2022

Hydrology and Earth System Sciences
Open Access
EGU
Discussions

Where the inflow perturbation is positive, the anomaly fraction increases for all scenarios across most of the thawing season (April to October) as flows are increasing. Where it is negative, as for *Glacier* the trend decreases in a similar time frame. The *Warming* scenario on the other hand continues to increase in anomaly fraction until November and experiences a sharp drop from April to May. In the freezing season (November to March), the *Combined* and *Permafrost* scenarios increase at first in November and December, but then begin a decreasing trend until March and April respectively. The *Glacier* scenario cannot be assessed in the freezing season because the inflow perturbation is zero.

Variability trends are largely consistent between *Glacier*, *Permafrost* and *Combined*. The variability tends to be higher in the late thawing season (July to October). The variability tends to be smaller in the freezing season when flows are lower. The *Warming* scenario is extremely variable in April and May.

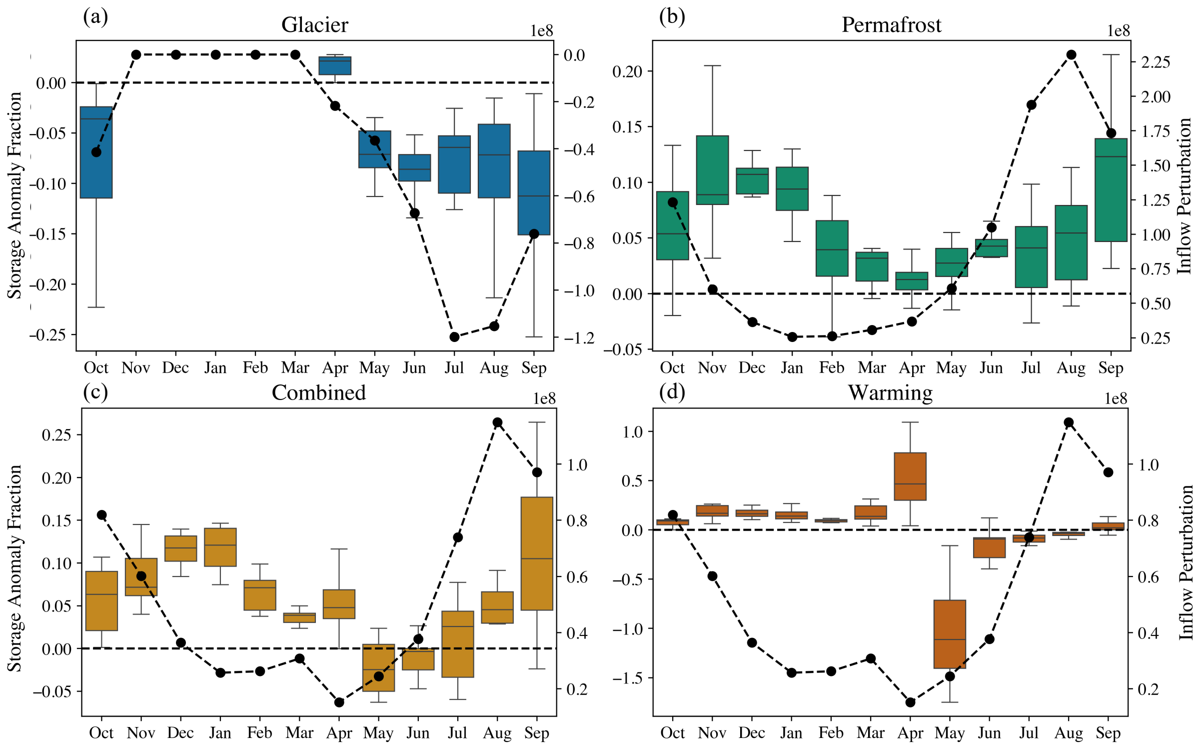

Figure 11: A boxplot of the monthly subsurface storage anomaly fraction for each scenario is shown. (a) is the Glacier scenario, (b) Permafrost, (c) Combined and (d) Warming. The colored box represents the interquartile range (IQR) and the line in the center of it is the mean storage anomaly in that month across all years of simulation. The whiskers extend from +/- 1.5IQR and cover 99.3% of the distribution. The outliers are not shown. Each point on the black dashed line is the average inflow perturbation in that month.

https://doi.org/10.5194/hess-2022-160
Preprint. Discussion started: 2 May 2022

Hydrology and Earth System Sciences
Discussions

3.4 The Impact of Warming

The *Combined* and *Warming* scenarios have the same inflow perturbations at the inlets (Figure 12, purple dots). However, the *Warming* scenario has 2C of warming relative to the temperatures in *Combined* applied across the entire simulation domain. When looking at evapotranspiration (ET), in the *Combined* scenario in January (Figure 12a), only small regions of ET are
440 greater relative to the *Baseline*. These regions are only in areas near the inlets. They are also more pronounced in areas which have higher flow, like the main steam of the Heihe.

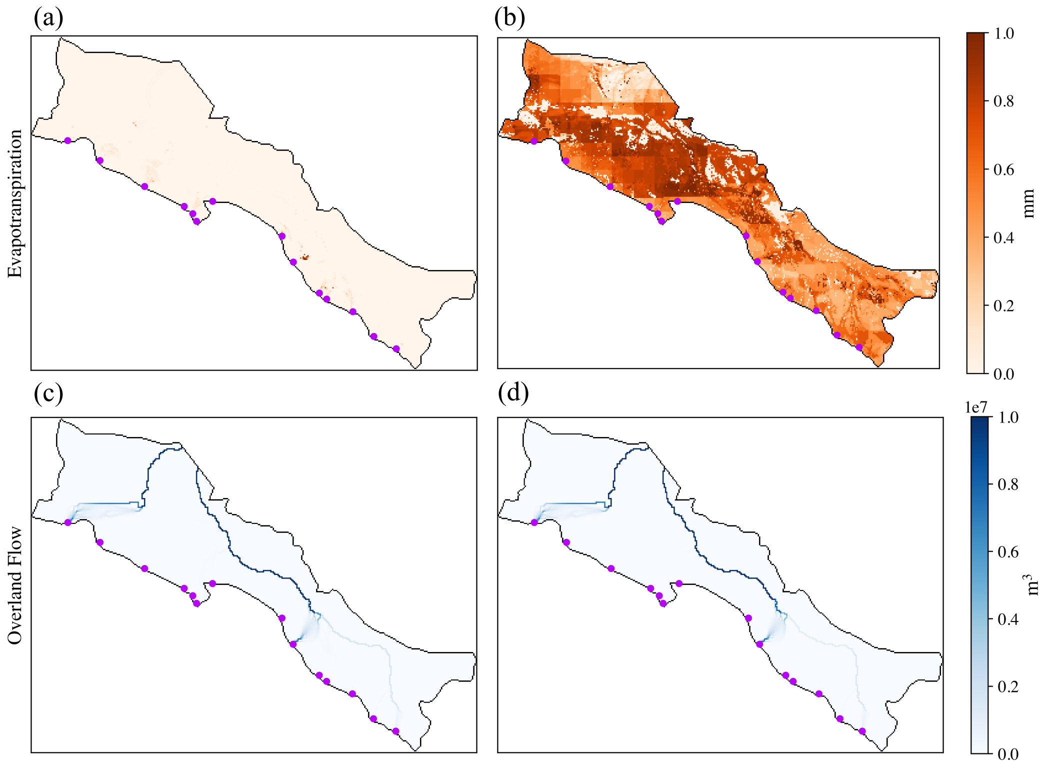

Figure 12: The difference of the average monthly sum in January of ET from Baseline for the Combined scenario (a) and Warming scenario (b). The difference in the sum of overland flow from Baseline is shown in (c) for Combined and (d) for Warming also for January.

The *Warming* scenario on the other hand shows large differences in ET across the domain relative to *Baseline*. These differences become more dramatic in July (Figure 13b) where the maximum ET difference almost quadruples. The differences
445 for the *Combined* scenario are also stronger and more widespread in July compared to January. It is now possible to see ET differences along the river channel into the domain, and not only near the inlets.

https://doi.org/10.5194/hess-2022-160
Preprint. Discussion started: 2 May 2022

Hydrology and Earth System Sciences
Discussions

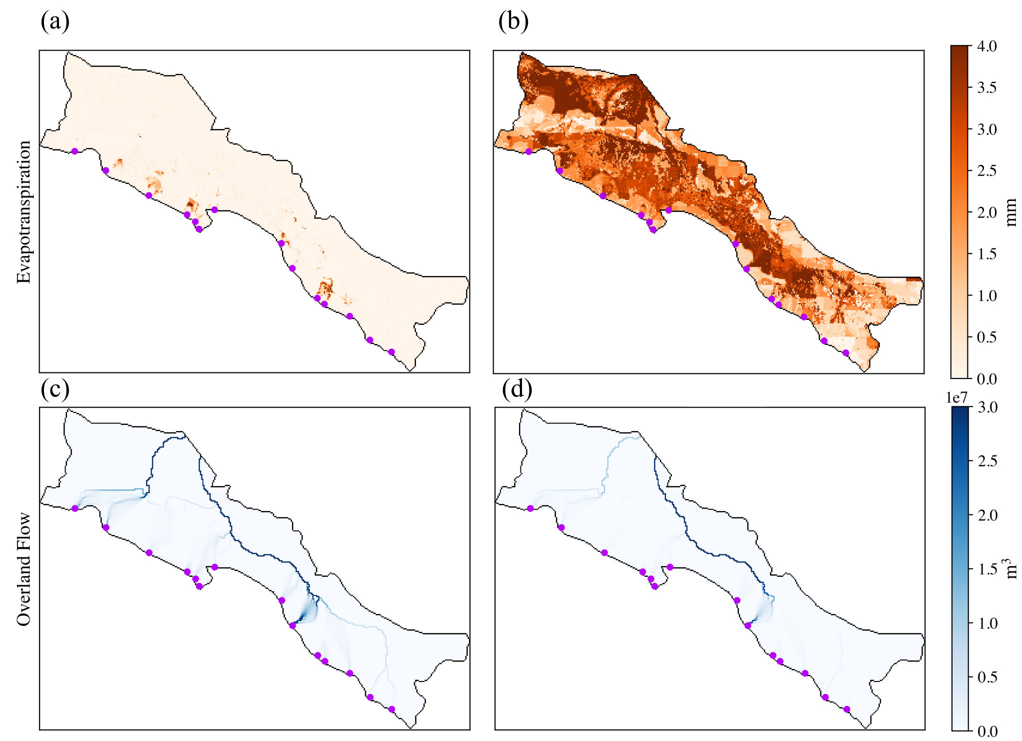

Figure 13: The difference of the average monthly sum in July of ET from Baseline for the Combined scenario (a) and Warming scenario (b). The difference in the sum of overland flow from Baseline is shown in (c) for Combined and (d) for Warming also for July.

The river network relative to *Baseline* also differs in January versus July. There is overall greater connectivity of tributaries and higher flows, especially in the *Combined* scenario. Additionally, while the river network between *Combined* and *Warming* looks very similar in January (12c and d), the river network as it compares to *Baseline* is noticeably different between them in July (13c and d). There is much less flow arriving at both the Heihe and Beide river outlets for *Warming*. There is also a significantly less connected river network in the lower right side of the domain compared to *Combined*.

The *Glacier* scenario (14a) has an increase in water table depth around the river inlets, although not as significant in magnitude as the rising water table in the *Permafrost* scenario (14b). The *Combined* (14a) and *Warming* (14b) scenarios show similar behavior with regards to rising water table near the river inlets. Several streams have a rise in water table greater than 20m near the boundary between the upper and middle Heihe relative to the *Baseline*. The areas of greatest increase are not necessarily directly adjacent to this boundary. The *Warming* scenario has broad areas across the domain where the water table has decreased by several meters. This is not seen in any other scenario and so is likely a result of warming.

https://doi.org/10.5194/hess-2022-160
Preprint. Discussion started: 2 May 2022

Hydrology and Earth System Sciences
Open Access
Discussions

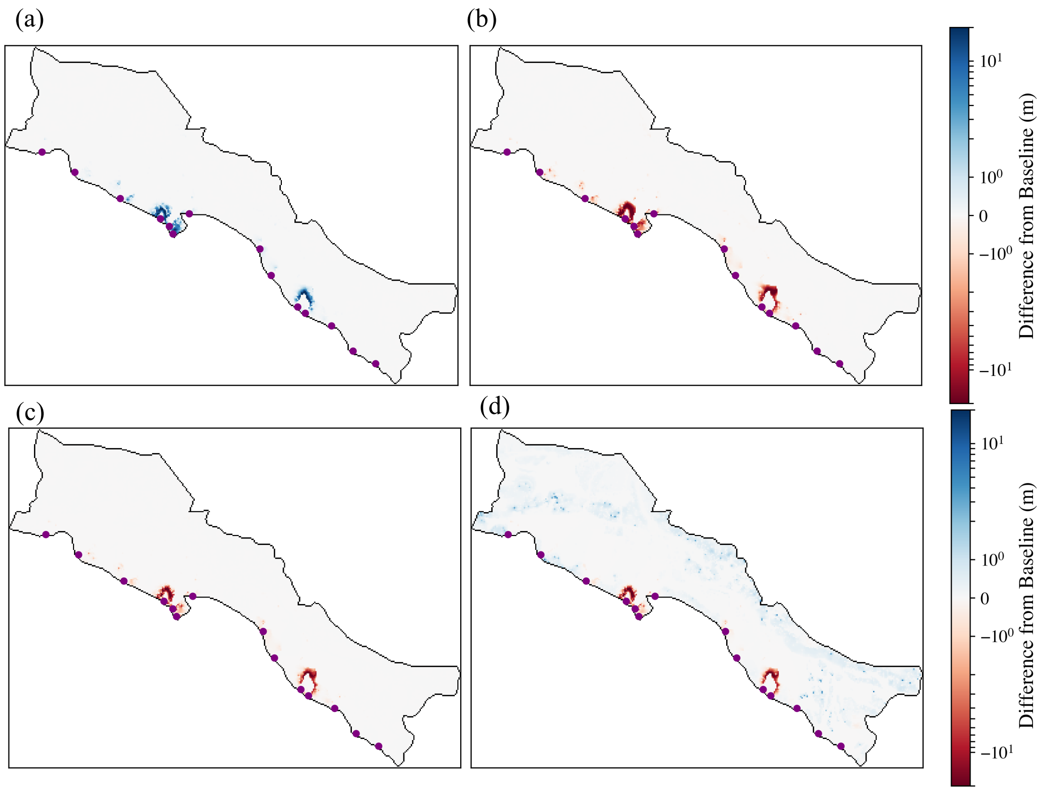

Figure 14: The difference in water table depth from Baseline after 11 years of simulation. (a) shows the Glacier scenario, (b) is the Permafrost scenario, (c) is the Combined scenario and (d) is the Warming scenario. The scale is in meters on a log scale, with red being increases in WTD and blue being decreases in WTD.

4 Discussion

4.1 Mediation of Cryosphere-based Streamflow Changes by the Middle Basin

First, we will explore the impacts from changes in the upper basin cryosphere (i.e., the *Glacier*, *Permafrost* and *Combined* scenarios) on the middle-basin. The *Glacier* scenario has an overall decrease in streamflow relative to *Baseline*, while the *Permafrost* scenario has an overall increase. Throughout all scenarios across all years (apart from 2011 for *Permafrost*), only a fraction of whatever change is applied at the inlet is still present at the outlet (Figure 7). When streamflow is decreased, stream height falls in the river channel resulting in increased baseflow from groundwater storage releasing to the stream (in locations where the groundwater is shallow and connected). The net result is that streamflow losses are compensated for by groundwater discharge resulting in a negative inflow perturbation at the inlet becoming less negative as we move

https://doi.org/10.5194/hess-2022-160
Preprint. Discussion started: 2 May 2022

Hydrology and Earth System Sciences
Open Access
EGU
Discussions

downstream to the outlet (Figure 6). When we increase flow, the opposite occurs (i.e., stream level increases can induce increased groundwater recharge or decrease groundwater discharge). Again, the net effect is a buffering of the streamflow perturbation, in this case the positive inlet perturbation decreasing as you move downstream to the outlet (Figure 6).

The buffering effect is largest in the first few years when the water table is at its greatest distance from the *Baseline* scenario. For the *Glacier* scenario, this means the most water leaving storage to augment streamflow and for the *Permafrost* scenario, this means the greatest amount of water added to storage. As the water table and stream height equilibrate, the gradient decreases and we expect smaller volumes of water to be exchanged. However, applied differences in streamflow with regards to the *Baseline* result in permanent differences in behavior between the scenarios as a new equilibrium is reached. After 2002, there is little shift in the rolling average of the anomaly fraction, this indicates that the system has approached a new equilibrium.

On average after 2002, 88%, 92% and 91% of the applied streamflow perturbation propagates downstream for *Glacier*, *Permafrost* and *Combined* respectively (Figure 7), while 8%, 5% and 5% of the perturbation is compensated for by changes in groundwater storage (Figure 10). This leaves 4%, 3% and 4% of the streamflow perturbation which may be compensated for by a shifting relationship with evapotranspiration. Figure 13b shows elevated evapotranspiration for the *Combined* scenario relative to *Baseline*, particularly near inlets and major river branches which supports this assessment.

Multiplying the storage anomaly fraction by the average annual inflow perturbation for each scenario allows us to estimate the total annual change in groundwater storage (note that the magnitude of the inflow perturbation varies across scenarios). We obtain a 39.5 million m^3 decrease of water each year for *Glacier*, an increase of 56.8 million m^3 for *Permafrost*, and an increase of 33.5 million m^3 for *Combined*. This means that the increase in baseflow from permafrost degradation will more than offset the reduction in flow from glacial loss as we see in the *Combined* scenario. It should also be noted that we selected an upper bound scenario for glacial flow reduction. So, it is highly likely that this is a conservative estimate, and that subsurface storage will increase in the future in the middle basin as a result of these two process changes.

Estimates of groundwater pumping in the middle basin can range anywhere from 220 million m^3 (Zeng et al., 2012) to 858.6 million m^3 per year (Tian et al., 2018). This is after adjusting for a groundwater being a presumed 30% of total water usage (Tian et al., 2018) and the middle basin accounting for 90% of water usage (Liu et al., 2009; Deng and Zhao, 2015). This results in a range of 3.32.9-15% of annual usage added to groundwater storage in the *Combined* scenario. This is likely to be highly impactful to human systems because the perturbation is applied to rivers, around which most human settlements and agriculture are located. However, this large uncertainty in groundwater usage estimates makes it difficult to assess the impact of these upstream inflow changes.

Watershed response to streamflow changes varies with the initial state of the water table. In the *Baseline* scenario, groundwater is already shallow across a large portion of the domain, especially near the stream (Figure 5). The areas of the domain with deep water tables at the start of simulation tend to be close to the boundary with the upper basin where there is a larger elevation gradient (Figure 1). This means that increased flows have a limited area within which to infiltrate and add significantly to storage compared to *Baseline*. This is seen in Figure 14a, which shows limited regions with a significant rise in water table. Saturated subsurface conditions combined with a high precipitation year result in the behavior illustrated in 2011 for *Permafrost*. Here, despite increased flows, less water is added to storage than the *Baseline* because a higher fraction of water is running off (Figure 9b, 10a). It is worth noting then that over time, permanent increases to subsurface storage may not be as significant as the increase in streamflow would suggest. However, if we consider the system with human impacts of pumping and diversion, it is possible we would continue to see streamflow supplement subsurface storage in a more stable way year after year.

4.2 Differences between the Heihe and Beide Rivers

The Heihe river drains most of the gaged tributaries (12) coming into the basin, while the Beide river in the Western part of the domain only drains two gaged tributaries before crossing into the lower basin (Figure 1). The result is a significantly smaller stream network for the Beide. Additionally, the distance from the inlet to outlet is on average shorter for branches of the Beide than Heihe river (Figure 1). Finally, there is a greater variation in water table depth around the tributaries of the Heihe than Beide (Figure 3). These factors combined result in different groundwater response to streamflow perturbation.

From 2003-2005 the inflow perturbation is always less than the outlet anomaly for the Beide River (Figure 6b) and after 2004 it switches to amplifying behavior (fraction greater than one) of the inflow perturbation signal (Figure 7b). The Heihe river shows dissimilar behavior where, with the exception of 2011 *Permafrost*, simulations always show dampening behavior (fraction less than one). In figure 14a, the two leftmost gages (purple markers), which drain to the Beide river, have little change in water table depth relative to *Baseline.* This implies that there is little ability for the streamflow signal to be buffered by interactions with groundwater storage. This would explain the lack of significant dampening behavior in the Beide, while for the Heihe we see dampening that is present but diminishing over time. There are several possible explanations for cases of amplifying behavior. First, in scenarios like *Permafrost* and *Combined* which have a net increase in flow, reduced infiltration of that signal over time as shallow groundwater storage fills results in increased runoff. In the *Glacier* scenario, where there is a reduction in flow, an amplification in this negative signal in the Beide may be due to falling water tables (Figure 14a) which induce further infiltration and streamflow losses (Figure 7b).

4.3 Seasonal Differences

The intra-annual behavior of the scenarios largely depends on if we are in a baseflow (winter and spring), or runoff (summer and fall) dominated month. In general, the applied streamflow perturbations are most dampened in the early thawing season and summer (i.e. the outlet anomaly fractions are smallest). For example, April is the month with the lowest outlet anomaly fraction for the *Glacier* scenario. In this month, on average about 50% of the streamflow reduction is buffered either by the release of groundwater from storage or reduced ET (Figure 8a). This is compared to September, where essentially none of the reduction is buffered, with a mean outlet anomaly fraction close to one (Figure 8a). Conversely, in scenarios where flow is increased relative to *Baseline*, such as *Permafrost* and *Combined*, the month with the smallest mean anomaly fractions occurs

https://doi.org/10.5194/hess-2022-160
Preprint. Discussion started: 2 May 2022

Hydrology and Earth System Sciences
Discussions

a little later (June for Permafrost and July for *Combined)*. Increased infiltration into the subsurface, or greater losses to evapotranspiration result in a larger fraction of the streamflow increase being lost before the basin outlet.

To determine if these differences in anomaly fraction are due to changing relationships with groundwater storage, we can look at Figure 11. First, for the *Glacier* scenario the only month with a positive fraction is April. In April, less storage is lost relative to Baseline than expected given the negative inflow perturbation. This is counterintuitive when considering the small outlet anomaly fraction (Figure 8a). However, the *Glacier* scenario has the same inflow as the *Baseline* during the freezing season, allowing for large increases in groundwater storage. The switch from a positive to negative fraction from April to May signifies that any surplus storage gained in the freezing season is lost by May. This accounts for the large dampening behavior in in April. The rest of the thawing season, the *Glacier* scenario gains less storage than the *Baseline*.

In the *Permafrost* and *Combined* scenarios, the storage anomaly tends to increase throughout the thawing and into the early freezing season (Figure 11). While the magnitude of the inflow perturbation is increasing, there is also an increase in the variability and range of the storage anomaly fraction. The variability tends to decrease in the freezing season, while the storage anomaly fraction remains high. Looking at July as an example (11b, c), depending on the year up to 10% of the inflow perturbation could be added to subsurface storage. However, in other years that fraction can be negative. That is, despite elevated flow over *Baseline*, less storage was added for the scenario. This is likely related to increasing flow across the thawing season. If subsurface storage near the stream network is fully saturated, then more of the inflow perturbation will pass through to the outlet and not infiltrate. This is reflected in outlet anomaly fractions approaching one across the thawing season (Figure 8). Regardless of if there is a decrease or increase in flow, at the end of the thawing season there is sufficient flow to saturate the subsurface adjacent to the stream network.

Storage anomaly fractions in the freezing season tend to be above zero and less variable (11b,c). Lower winter flows result in a smaller likelihood of oversaturating the subsurface near the river network. Second, lower connectivity of tributaries to the main stem during this low flow period increase the amount of streamflow that infiltrates before arriving at the outlet. This second point can be visualized with differences in river network connectivity between January and July (Figure 12c, 13c). This means that changes to subsurface storage are more consistent in the freezing season. Ultimately, permafrost mediated changes to baseflow will have a more consistent impact on groundwater storage in the freezing than thawing season.

4.4 The Influence of Warming Temperature

Increasing the temperature in the middle basin changes many of the overall impacts of the *Combined* scenario discussed in previous sections. Changes to streamflow impact water table depth and ET in a limited area of the domain (Figure 14). *Warming* the domain on the other hand, will impact the entire middle basin. In figure 13b ET is elevated across the domain compared to the *Baseline*. Increases in ET across the domain in the *Warming scenario* result in visibly lower flows in the main river stems, and loss of connection of smaller tributaries in the *Warming* scenario compared to *Combined,* even though they have identical inflows (Figure 13 a, b). Impacts are less pronounced in January (Figure 12 a, b) when ET is lower.

https://doi.org/10.5194/hess-2022-160
Preprint. Discussion started: 2 May 2022

Hydrology and Earth System Sciences
Open Access
EGU
Discussions

Increased ET reduces shallow groundwater storage and decreases the chance of completely saturating the subsurface during high flow summer periods. These two factors combined cause dampening behavior to persist throughout the simulation period for the *Warming* scenario. For example, in Figure 6a,b both major rivers have consistent dampening behavior in each year of simulation. This is not the case for the *Combined* scenario which switches to amplifying behavior in the Beide and is variable in the Heihe. Likewise for the outlet anomaly fraction, more than 80% of the flow increase is never present at the outlet for the Heihe river (Figure 7a). Less runoff reaching the stream network due to increased ET also contributes to this result.

The *Warming* scenario also has a small net loss in subsurface storage (equating to about .24% of annual use) (Figure 10a and Figure 14d). This is due to the diffuse, small drops in WTD throughout the domain. The *Warming* scenario does have a similar rise in water table near the river inlets as in the *Combined* scenario (Figure 14c and d) which does not fully counteract the losses in subsurface storage. The *Warming* scenario also has more variable and negative fractions compared to *Combined* in the shallow subsurface (Figure 10c). Additionally, less water available to infiltrate results in a steady declining trend in the deep subsurface overtime (Figure 10b). If we assume that rising WTD and increasing groundwater storage near the inlets slows down overtime as indicated, reductions in groundwater storage due to warming may be more significant relative to *Baseline* than they appear initially.

The *Warming* scenario also shows markedly different behavior than the *Combined* scenario in the spring. In April and May when streamflow increase at the inlet are small, increases in ET are larger than the streamflow perturbations (Figure 8d). As a result, the net impact is a streamflow decrease at the outlet relative to *Baseline.* The warming scenario also gains less storage compared to *Baseline* throughout the summer, rarely showing increases in subsurface storage relative to *Baseline* until October (Figure 11d). This differs from the *Combined* scenario which shows relative increases to subsurface storage starting in July (Figure 11c). The behavior between the two scenarios for both the outlet and storage anomaly is similar in the freezing season where the impact of increased ET, even with 2C warming, is minimal. Ultimately, the benefits of a higher flow regime will not be as strong in the middle basin in conjunction with the impacts of warming.

4.5 Caveats

We have made several simplifying assumptions throughout this research in order to design a well constrained experiment. However, these assumptions may also influence our findings. We briefly discuss three principal assumptions in our research and how they may impact our results. First, we model a natural flow state even though the middle basin is subject to intensive surface and groundwater usage. Our results are valuable to understanding the physical processes and progression of upstream flow changes on the middle basin. However, these impacts will change when modeled with water usage. Next, we only looked at perturbations to streamflow related to temperature changes in the upper basin. There are other processes that may occur under future climate change which we did not address such as precipitation changes. However, precipitation trends are less predictable and difficult to disentangle from increasing baseflow due to permafrost degradation. Last, it would be valuable to

https://doi.org/10.5194/hess-2022-160
Preprint. Discussion started: 2 May 2022

Hydrology and Earth System Sciences Discussions

run the model for a longer period. This would allow for a better analysis of the long-term response of groundwater storage to changing streamflow. However, we do remain constrained by data availability.

There are two main ways we would like to expand upon this work. First, adding water management operations in the middle basin would give a more realistic view of how these changes will impact the modern basin. While the physical processes are unlikely to change, the magnitude of the impact will shift. Second, it would be ideal to link middle basin domain to a model of the upper basin. That way, glacial melt and permafrost degradation would not be simplified and could be linked directly to processes modeled in the middle basin. This would allow for a more physically based change in flow timing and magnitude.

5 Conclusion

Climate warming in the upper basin cryosphere is essentially inevitable. The disappearance of glaciers will decrease overall streamflow, while permafrost degradation will increase baseflow. Examining the downstream impact on an ecologically and economically important region, such as the middle basin of the Heihe, is of critical importance. Through targeted changes to upper basin discharge and middle basin temperature, this study informs future impact to water resources in the middle basin.

Overall, our results indicate that there will likely be an increase in streamflow and groundwater storage from combined changes to discharge coming out of the cryosphere. Additionally, even when reductions are severe such as in the Glacier scenario, impacts to middle basin water supply are not as extreme. Groundwater exchanges can mediate some of the short-term impacts and dampen the overall shift. However, the warming impacts on the middle basin may be more dramatic than the shifts to streamflow. We find that widespread warming can overwhelm the streamflow shifts occurring in the upper basin through increasing ET which thereby reduces streamflow and groundwater storage in the middle basin. Our findings are relevant to other semi-arid basins with mountainous water sources that are facing uncertainty and water stress under climate warming.

Code and Data Availability

All data and programming scripts used to produce this work can be found on Cyverse under the following DOI: https://doi.org/10.25739/kmk7-b046. Any data or scripts not included in this repository can be made available upon request. Finally, any source data that is not specifically attributed in the manuscript can be accessed at the Heihe Program Data Management Center (http://heihedata.org).

Author Contribution

AT under the advisement of LC built the model as well as designing and running the scenarios. AT also analyzed all data and created all figures with feedback and guidance from LC. AT wrote the manuscript with revising and editing provided by LC.

Competing Interests

The authors declare that they have no conflict of interest.

Acknowledgments

The authors would like to thank the National Science Foundation (Award number 1855912) for funding all aspects of this project. Additionally, our gratitude to our collaborators at Southern University of Science and Technology, particularly Dr. Yong Tian, who was integral in providing source data and information about the Heihe River Basin.

References

Ashby, S. F., and Falgout, R. D.: A Parallel Multigrid Preconditioned Conjugate Gradient Algorithm for Groundwater Flow Simulations, Nuclear Science and Engineering, 124, 145-159, 10.13182/NSE96-A24230, 1996.

Carey, S. K., and Woo, M.-K.: Slope runoff processes and flow generation in a subarctic, subalpine catchment, Journal of Hydrology, 253, 110-129, 2001.

Chen, R., Wang, G., Yang, Y., Liu, J., Han, C., Song, Y., Liu, Z., and Kang, E.: Effects of Cryospheric Change on Alpine Hydrology: Combining a Model With Observations in the Upper Reaches of the Hei River, China, Journal of Geophysical Research: Atmospheres, 123, 3414-3442, 10.1002/2017jd027876, 2018.

Chen, Y., Zhang, D., Sun, Y., Liu, X., Wang, N., and Savenije, H. H. G.: Water demand management: A case study of the Heihe River Basin in China, Physics and Chemistry of the Earth, Parts A/B/C, 30, 408-419, 10.1016/j.pce.2005.06.019, 2005.

Chen, Y.: Water Resources Research in Northwest China, 1-444 pp., 2014.

Chen, Y., Li, Z., Fan, Y., Wang, H., and Deng, H.: Progress and prospects of climate change impacts on hydrology in the arid region of northwest China, Environ Res, 139, 11-19, 10.1016/j.envres.2014.12.029, 2015.

Condon, L. E., and Maxwell, R. M.: Feedbacks between managed irrigation and water availability: Diagnosing temporal and spatial patterns using an integrated hydrologic model, Water Resources Research, 50, 2600-2616, 10.1002/2013wr014868, 2014.

Condon, L. E., and Maxwell, R. M.: Modified priority flood and global slope enforcement algorithm for topographic processing in physically based hydrologic modeling applications, Computers & Geosciences, 126, 73-83, 10.1016/j.cageo.2019.01.020, 2019.

Condon, L. E., Atchley, A. L., and Maxwell, R. M.: Evapotranspiration depletes groundwater under warming over the contiguous United States, Nat Commun, 11, 873, 10.1038/s41467-020-14688-0, 2020.

Deng, X., and Zhao, C.: Identification of Water Scarcity and Providing Solutions for Adapting to Climate Changes in the Heihe River Basin of China, Advances in Meteorology, 2015, 1-13, 10.1155/2015/279173, 2015.

Ferguson, I. M., and Maxwell, R. M.: Role of groundwater in watershed response and land surface feedbacks under climate change, Water Resources Research, 46, 10.1029/2009wr008616, 2010.

Foster, L. M., and Maxwell, R. M.: Sensitivity analysis of hydraulic conductivity and Manning's n parameters lead to new method to scale effective hydraulic conductivity across model resolutions, Hydrological Processes, 33, 332-349, 10.1002/hyp.13327, 2018.

Gao, B., Yang, D., Qin, Y., Wang, Y., Li, H., Zhang, Y., and Zhang, T.: Change in frozen soils and its effect on regional hydrology, upper Heihe basin, northeastern Qinghai–Tibetan Plateau, The Cryosphere, 12, 657-673, 10.5194/tc-12-657-2018, 2018.

Gilbert, J. M., and Maxwell, R. M.: Examining regional groundwater–surface water dynamics using an integrated hydrologic model of the San Joaquin River basin, Hydrology and Earth System Sciences, 21, 923-947, 10.5194/hess-21-923-2017, 2017.

Gilbert, J. M., and Maxwell, R. M.: Contrasting warming and drought in snowmelt-dominated agricultural basins: revealing the role of elevation gradients in regional response to temperature change, Environmental Research Letters, 13, 10.1088/1748-9326/aacb38, 2018.

Gleeson, T., Moosdorf, N., Hartmann, J., and van Beek, L. P. H.: A glimpse beneath earth's surface: GLobal HYdrogeology MaPS (GLHYMPS) of permeability and porosity, Geophysical Research Letters, 41, 3891-3898, 10.1002/2014gl059856, 2014.
Gochis, D. J., Yu, W., and Yates, D. N.: The WRF-Hydro model technical description and user's guide, version 3.0. NCAR Technical Document. , 120 pages, Available online at: http://www.ral.ucar.edu/projects/wrf_hydro/, 2015.
Han, F., Zheng, Y., Tian, Y., Li, X., Zheng, C., and Li, X.: Accounting for field-scale heterogeneity in the ecohydrological modeling of large arid river basins: Strategies and relevance, Journal of Hydrology, 595, 10.1016/j.jhydrol.2021.126045, 2021.
He, J., Yang, K., Tang, W., Lu, H., Qin, J., Chen, Y., and Li, X.: The first high-resolution meteorological forcing dataset for land process studies over China, Scientific Data, 7, 25, 10.1038/s41597-020-0369-y, 2020.
He, J. Q., Song, G. J., Jiang, X., Li, Q. L., and Wu, X. B.: Relation between glacial meltwater runoff and mountainous runoff in 2006 in four typical river basins of Heihe river water system, Journal of Desert Research, 28, 1186-1190 (In Chinese), 2008.
Hein, A., Condon, L. E., and Maxwell, R. M.: Evaluating the relative importance of precipitation, temperature and land-cover change in the hydrologic response to extreme meteorological drought conditions over the North American High Plains, Hydrology and Earth System Sciences, 23, 1931-1950, 10.5194/hess-23-1931-2019, 2019.
Hu, X., Lu, L., Li, X., Wang, J., and Guo, M.: Land Use/Cover Change in the Middle Reaches of the Heihe River Basin over 2000-2011 and Its Implications for Sustainable Water Resource Management, PLoS One, 10, e0128960, 10.1371/journal.pone.0128960, 2015.
Huntington, J. L., and Niswonger, R. G.: Role of surface-water and groundwater interactions on projected summertime streamflow in snow dominated regions: An integrated modeling approach, Water Resources Research, 48, 10.1029/2012wr012319, 2012.
IPCC: Climate Change 2014: Synthesis Report. Contribution of Working Groups I, II, and III to the Fifth Assessment Report of the Intergovernmental Panel on Climate Change [Core Writing Team, R.K. Pachauri and L.A. Meyer (eds.)], IPCC, Geneva, Switzerland, 151 pp., 2014.
Jones, J. B., and Rinehart, A. J.: The long-term response of stream flow to climatic warming in headwater streams of interior Alaska, Canadian Journal of Forest Research, 40, 1210-1218, 10.1139/x10-047, 2010.
Jones, J. E., and Woodward, C. S.: Newton-Krylov-multigrid solvers for large-scale, highly heterogenous, variably saturated flow problems, Advances in Water Resources, 24, 763-774, https://doi.org/10.1016/S0309-1708(00)00075-0, 2001.
Kang, E., Cheng, G., Lan, Y., and Jin, H.: A model for simulating the response of runoff from the mountainous watersheds of inland river basins in the arid area of northwest China to climatic changes, Science in China Series D: Earth Sciences, 42, 52-63, 1999.
Kollet, S. J., and Maxwell, R. M.: Integrated surface–groundwater flow modeling: A free-surface overland flow boundary condition in a parallel groundwater flow model, Advances in Water Resources, 29, 945-958, 10.1016/j.advwatres.2005.08.006, 2006.
Kollet, S. J., and Maxwell, R. M.: Capturing the influence of groundwater dynamics on land surface processes using an integrated, distributed watershed model, Water Resources Research, 44, 10.1029/2007wr006004, 2008.
Liu, B., Zhao, W., Chang, X., Li, S., Zhang, Z., and Du, M.: Water requirements and stability of oasis ecosystem in arid region, China, Environmental Earth Sciences, 59, 1235-1244, 10.1007/s12665-009-0112-7, 2009.
Liu, Y., Hao, L., Zhou, D., Pan, C., Liu, P., Xiong, Z., and Sun, G.: Identifying a transition climate zone in an arid river basin using the evaporative stress index, Natural Hazards and Earth System Sciences, 19, 2281-2294, 10.5194/nhess-19-2281-2019, 2019a.
Liu, Z., Liu, S., Ye, J., Sheng, F., You, K., Xiong, X., and Lai, G.: Application of a Digital Filter Method to Separate Baseflow in the Small Watershed of Pengchongjian in Southern China, Forests, 10, 10.3390/f10121065, 2019b.
Lu, Z., Wei, Y., Xiao, H., Zou, S., Xie, J., Ren, J., and Western, A.: Evolution of the human–water relationships in the Heihe River basin in the past 2000 years, Hydrology and Earth System Sciences, 19, 2261-2273, 10.5194/hess-19-2261-2015, 2015.
Ma, Q., Jin, H.-J., Bense, V. F., Luo, D.-L., Marchenko, S. S., Harris, S. A., and Lan, Y.-C.: Impacts of degrading permafrost on streamflow in the source area of Yellow River on the Qinghai-Tibet Plateau, China, Advances in Climate Change Research, 10, 225-239, 10.1016/j.accre.2020.02.001, 2019.
Markstrom, S. L., Niswonger, R. G., Regan, S. R., Prudic, D. E., and Barlow, P. M.: GSFLOW - coupled ground-water and surface-water flow model based on the integration of the precipitation-runoff modeling system (PRMS) and the modular

ground-water flow model (MODFLOW-2005), U.S. Geoological Survey Techniques and Methods 6-D1, Chapter 1, Section D, Book 6, 2008.

Maxwell, R. M., and Miller, N. L.: Development of a Coupled Land Surface and Groundwater Model, Journal of Hydrometeorology, 6, 233-247, https://doi.org/10.1175/JHM422.1, 2005.

Maxwell, R. M.: A terrain-following grid transform and preconditioner for parallel, large-scale, integrated hydrologic modeling, Advances in Water Resources, 53, 109-117, 10.1016/j.advwatres.2012.10.001, 2013.

Maxwell, R. M., Condon, L. E., and Kollet, S. J.: A high-resolution simulation of groundwater and surface water over most of the continental US with the integrated hydrologic model ParFlow v3, Geoscientific Model Development, 8, 923-937, 10.5194/gmd-8-923-2015, 2015.

Niu, L., Ye, B., Li, J., and Sheng, Y.: Effect of permafrost degradation on hydrological processes in typical basins with various permafrost coverage in Western China, Science China Earth Sciences, 54, 615-624, 10.1007/s11430-010-4073-1, 2010.

Qin, D., Zhou, B., and Xiao, C.: Progress in studies of cryospheric changes and their impacts on climate of China, Journal of Meteorological Research, 28, 732-746, 10.1007/s13351-014-4029-z, 2014.

Qin, J., Ding, Y., and Yang, G.: The hydrological linkage of mountains and plains in the arid region of northwest China, Chinese Science Bulletin, 58, 3140-3147, 10.1007/s11434-013-5768-4, 2013.

Shi, Y., Shen, Y., Kang, E., Li, D., Ding, Y., Zhang, G., and Hu, R.: Recent and Future Climate Change in Northwest China, Climatic Change, 80, 379-393, 10.1007/s10584-006-9121-7, 2006.

Song, C., Wang, G., Mao, T., Dai, J., and Yang, D.: Linkage between permafrost distribution and river runoff changes across the Arctic and the Tibetan Plateau, Science China Earth Sciences, 63, 292-302, 10.1007/s11430-018-9383-6, 2019.

Sun, T., Wang, J., Huang, Q., and Li, Y.: Assessment of Water Rights and Irrigation Pricing Reforms in Heihe River Basin in China, Water, 8, 10.3390/w8080333, 2016.

Sun, Z., Zheng, Y., Li, X., Tian, Y., Han, F., Zhong, Y., Liu, J., and Zheng, C.: The Nexus of Water, Ecosystems, and Agriculture in Endorheic River Basins: A System Analysis Based on Integrated Ecohydrological Modeling, Water Resources Research, 54, 7534-7556, 10.1029/2018wr023364, 2018.

Thatch, L. M., Gilbert, J. M., and Maxwell, R. M.: Integrated Hydrologic Modeling to Untangle the Impacts of Water Management During Drought, Ground Water, 58, 377-391, 10.1111/gwat.12995, 2020.

Tian, Y., Zheng, Y., Wu, B., Wu, X., Liu, J., and Zheng, C.: Modeling surface water-groundwater interaction in arid and semi-arid regions with intensive agriculture, Environmental Modelling & Software, 63, 170-184, 10.1016/j.envsoft.2014.10.011, 2015a.

Tian, Y., Zheng, Y., Zheng, C., Xiao, H., Fan, W., Zou, S., Wu, B., Yao, Y., Zhang, A., and Liu, J.: Exploring scale-dependent ecohydrological responses in a large endorheic river basin through integrated surface water-groundwater modeling, Water Resources Research, 51, 4065-4085, 10.1002/2015wr016881, 2015b.

Tian, Y., Xiong, J., He, X., Pi, X., Jiang, S., Han, F., and Zheng, Y.: Joint Operation of Surface Water and Groundwater Reservoirs to Address Water Conflicts in Arid Regions: An Integrated Modeling Study, Water, 10, 10.3390/w10081105, 2018.

Viviroli, D., and Weingartner, R.: The hydrological significance of mountains: from regional to global scale, Hydrology and Earth System Sciences, 8, 1016-1029, 2004.

Viviroli, D., Archer, D. R., Buytaert, W., Fowler, H. J., Greenwood, G. B., Hamlet, A. F., Huang, Y., Koboltschnig, G., Litaor, M. I., López-Moreno, J. I., Lorentz, S., Schädler, B., Schreier, H., Schwaiger, K., Vuille, M., and Woods, R.: Climate change and mountain water resources: overview and recommendations for research, management and policy, Hydrology and Earth System Sciences, 15, 471-504, 10.5194/hess-15-471-2011, 2011.

Walvoord, M. A., and Striegl, R. G.: Increased groundwater to stream discharge from permafrost thawing in the Yukon River basin: Potential impacts on lateral export of carbon and nitrogen, Geophysical Research Letters, 34, 10.1029/2007gl030216, 2007.

Wang, G. X., and Cheng, G. D.: The characteristics of water resources and the changes of the hydrological process and environment in the arid zone of northwest China, Environmental Geology, 39, 783-790, 2000.

Wu, F., Zhan, J., Wang, Z., and Zhang, Q.: Streamflow variation due to glacier melting and climate change in upstream Heihe River Basin, Northwest China, Physics and Chemistry of the Earth, Parts A/B/C, 79-82, 11-19, 10.1016/j.pce.2014.08.002, 2015.

Xiong, Z., and Yan, X.: Building a high-resolution regional climate model for the Heihe River Basin and simulating precipitation over this region, Chinese Science Bulletin, 58, 4670-4678, https://doi.org/10.1007/s11434-013-5971-3, 2013.

https://doi.org/10.5194/hess-2022-160
Preprint. Discussion started: 2 May 2022

Hydrology and Earth System Sciences
Discussions

Xu, M., Kang, S., and Li, J.: Evaluation of Water Storage Change of Inland Cryosphere in Northwestern China, Advances in Meteorology, 2015, 1-12, 10.1155/2015/681634, 2015.

Yang, Z. N.: Glacier Water Resources in China, Gansu Science and Technology Press, 1991.

Yao, Y., Zheng, C., Liu, J., Cao, G., Xiao, H., Li, H., and Li, W.: Conceptual and numerical models for groundwater flow in an arid inland river basin, Hydrological Processes, 29, 1480-1492, 10.1002/hyp.10276, 2015a.

Yao, Y., Zheng, C., Tian, Y., Liu, J., and Zheng, Y.: Numerical modeling of regional groundwater flow in the Heihe River Basin, China: Advances and new insights, Science China Earth Sciences, 58, 3-15, 10.1007/s11430-014-5033-y, 2015b.

Yao, Y., Tian, Y., Andrews, C., Li, X., Zheng, Y., and Zheng, C.: Role of Groundwater in the Dryland Ecohydrological System: A Case Study of the Heihe River Basin, Journal of Geophysical Research: Atmospheres, 123, 6760-6776, 10.1029/2018jd028432, 2018.

Ye, B., Yang, D., Zhang, Z., and Kane, D. L.: Variation of hydrological regime with permafrost coverage over Lena Basin in Siberia, Journal of Geophysical Research, 114, 10.1029/2008jd010537, 2009.

You, Q., Wu, T., Shen, L., Pepin, N., Zhang, L., Jiang, Z., Wu, Z., Kang, S., and AghaKouchak, A.: Review of snow cover variation over the Tibetan Plateau and its influence on the broad climate system, Earth-Science Reviews, 201, 10.1016/j.earscirev.2019.103043, 2020.

Zeng, Z., Liu, J., Koeneman, P. H., Zarate, E., and Hoekstra, A. Y.: Assessing water footprint at river basin level: a case study for the Heihe River Basin in northwest China, Hydrology and Earth System Sciences, 16, 2771-2781, 10.5194/hess-16-2771-2012, 2012.

Zhang, A., Zheng, C., Wang, S., and Yao, Y.: Analysis of streamflow variations in the Heihe River Basin, northwest China: Trends, abrupt changes, driving factors and ecological influences, Journal of Hydrology: Regional Studies, 3, 106-124, 10.1016/j.ejrh.2014.10.005, 2015a.

Zhang, A., Liu, W., Yin, Z., Fu, G., and Zheng, C.: How Will Climate Change Affect the Water Availability in the Heihe River Basin, Northwest China?, Journal of Hydrometeorology, 17, 1517-1542, 10.1175/jhm-d-15-0058.1, 2016.

Zhang, L., Nan, Z., Yu, W., and Ge, Y.: Modeling Land-Use and Land-Cover Change and Hydrological Responses under Consistent Climate Change Scenarios in the Heihe River Basin, China, Water Resources Management, 29, 4701-4717, 10.1007/s11269-015-1085-9, 2015b.

Zhang, Y., Xu, C.-Y., Hao, Z., Zhang, L., Ju, Q., and Lai, X.: Variation of Melt Water and Rainfall Runoff and Their Impacts on Streamflow Changes during Recent Decades in Two Tibetan Plateau Basins, Water, 12, 10.3390/w12113112, 2020.

Zhao, W., Li, Z. L., and Wang, Y. H.: Separation and characteristics of base flow in the upper reaches of Heihe River Basin, South North Water Transf. Water Sci. Tech., 14, 26-31 (In Chinese), 2016.

Zongxing, L., Qi, F., Wang, Q. J., Song, Y., Hongyi, L., and Yongge, L.: The influence from the shrinking cryosphere and strengthening evopotranspiration on hydrologic process in a cold basin, Qilian Mountains, Global and Planetary Change, 144, 119-128, 10.1016/j.gloplacha.2016.06.017, 2016.